RESEARCH ARTICLE

A model of dopamine and serotonin-kynurenine metabolism in cortisolemia: Implications for depression

Felipe Dalvi-Garcia[1,2]*, **Luis L. Fonseca**[3], **Ana Tereza R. Vasconcelos**[1], **Cecilia Hedin-Pereira**[4,5], **Eberhard O. Voit**[3]

1 Bioinformatics Lab, National Laboratory for Scientific Computing, Petrópolis, Rio de Janeiro, Brazil, **2** School of Medicine and Surgery, Federal University of the State of Rio de Janeiro, Rio de Janeiro, Rio de Janeiro, Brazil, **3** Department of Biomedical Engineering, Georgia Institute of Technology, Atlanta, Georgia, United States of America, **4** Center of Health Sciences, Federal University of Rio de Janeiro, Rio de Janeiro, Rio de Janeiro, Brazil, **5** Oswaldo Cruz Institute, Oswaldo Cruz Foundation, Rio de Janeiro, Rio de Janeiro, Brazil

* felipedalvi@edu.unirio.br

Abstract

A major factor contributing to the etiology of depression is a neurochemical imbalance of the dopaminergic and serotonergic systems, which is caused by persistently high levels of circulating stress hormones. Here, a computational model is proposed to investigate the interplay between dopaminergic and serotonergic-kynurenine metabolism under cortisolemia and its consequences for the onset of depression. The model was formulated as a set of nonlinear ordinary differential equations represented with power-law functions. Parameter values were obtained from experimental data reported in the literature, biological databases, and other general information, and subsequently fine-tuned through optimization. Model simulations predict that changes in the kynurenine pathway, caused by elevated levels of cortisol, can increase the risk of neurotoxicity and lead to increased levels of 3,4-dihydroxyphenylaceltahyde (DOPAL) and 5-hydroxyindoleacetaldehyde (5-HIAL). These aldehydes contribute to alpha-synuclein aggregation and may cause mitochondrial fragmentation. Further model analysis demonstrated that the inhibition of both serotonin transport and kynurenine-3-monooxygenase decreased the levels of DOPAL and 5-HIAL and the neurotoxic risk often associated with depression. The mathematical model was also able to predict a novel role of the dopamine and serotonin metabolites DOPAL and 5-HIAL in the ethiology of depression, which is facilitated through increased cortisol levels. Finally, the model analysis suggests treatment with a combination of inhibitors of serotonin transport and kynurenine-3-monooxygenase as a potentially effective pharmacological strategy to revert the slow-down in monoamine neurotransmission that is often triggered by inflammation.

Author summary

According to the World Health Organization, major depressive disorder (MDD) was in 2014 the fourth leading cause of disability in people between the ages of 15 and 44 years.

MDD is responsible for about 1 million suicides per year and associated with a number of other medical conditions such as coronary disease, diabetes, and Alzheimer's disease. While MDD has been studied for a long time, molecular details of its pathophysiology are still scarce. Computational models offer a powerful opportunity to assist neuropsychiatric disorder research, as they permit the representation of large sets of physiological, cellular and biochemical phenomena through mathematical equations that can be simulated in a very efficient fashion and have the capacity to provide testable hypotheses. Here, we introduce a computational model of relevant biochemical pathways associated with high levels of circulating stress hormone, as they are observed in MDD. The model captures known observations well and demonstrates how increased levels of internally produced toxic agents, such as various kynurenines, DOPAL and 5-HIAL, can lead to dysregulation of key enzymes. These insights suggest new hypotheses for model-driven experiments, as well as novel potential targets for pharmacological intervention.

Introduction

Affective disorders alter the mood of an individual. According to the Diagnostic and Statistical Manual of Mental Disorders-V, these disorders are typically classified as depressive or bipolar [1] if they are pathological or intense and persistent. Most common among them is major depressive disorder (MDD). Its symptoms include depressive mood, anhedonia, reduced energy, feelings of guilt and/or low self-esteem, sleep problems, changes in appetite, irritability, lack of concentration and bouts of anxiety [2].

According to the World Health Organization, MDD is responsible for about 1 million suicides per year and expected to be the second leading cause of disability in 2020 and the first in 2040 [2,3]. Research during the past decade has focused on links between depression and the development of other medical conditions, such as coronary heart disease [4], diabetes [5] and Alzheimer's disease [6]. Up to 64% of recovered patients may suffer recurrent episodes of MDD [7], and only about 30 to 35% of adults treated with antidepressants go into remission [8]. Despite these disturbing statistics and the considerable impact of MDD on health and society, the biological basis for the pathophysiology of MDD is still obscure [9].

Different biochemical theories have suggested that imbalances in the levels of biogenic amines, such as dopamine (DA) and serotonin (5-HT), are involved in the etiology of psychiatric disorders like schizophrenia, attention-deficit/hyperactivity disorder, and depression [10–14]. These imbalances in dopaminergic and serotonergic systems are, in turn, likely to affect the chemical balance within the entire neurotransmitter system [15,16] and, as a consequence, are presumably not the only causes for depression. Instead, factors beyond changes in the metabolism of these monoamines likely contribute to the pathogenesis of MDD as well. As a pertinent example, many studies have shown that the influence of persistent, high levels of circulating stress hormones can be a potent trigger of MDD [17,18]. Cortisol (CORT) in humans, or corticosterone in rodents, is one of the hormones that have been directly associated with decreases in dopamine and serotonin levels. The subsequent imbalances in neurotransmission can have different outcomes, depending on the affected brain regions [19].

Impairments in neurotransmitter metabolism due to changes in CORT have been reported to play a key role in the prefrontal cortex (PFC) and can lead to the development of MDD [20–22]. One reason is neuroanatomical: dopaminergic and serotonergic cell bodies are located in other regions, but their nerve terminals are projected towards the PFC where they interact with each other. These terminals possess the entire necessary cellular machinery for synthesis, release, reuptake and degradation of neurotransmitters [23]. As a result, the overlap in

dopaminergic and serotonergic axon terminals in the PFC and their metabolic autonomy are important features that suggest a focused investigation of these terminals toward a deeper understanding of the neurochemical processes that are involved in the onset of MDD.

Another contributor to MDD appears to be the kynurenine (KYN) pathway (KP), which constitutes a side branch of tryptophan metabolism through which tryptophan can be channeled away from the serotonin pathway. Although KYN was discovered at the end of the 19th century, long before serotonin, KYN and its metabolites have received increased attention only during the past decade, particularly due to their links to inflammation, the immune system and a variety of neurological conditions [24]. Moreover, it has been reported that KYN derivatives can impair the metabolism of aldehydes that result from the catabolism of dopamine and serotonin, and furthermore regulate glutamate neurotransmission by affecting the N-methyl-D-aspartate (NMDA) receptor [25,26].

Over the years, animal models have been used to study the neuropathophysiology of psychiatric disorders, such as MDD [14]. In particular, the association between stress and the etiology of depression has been investigated with experiments that induce depressive behavior by increasing the level of CORT in an animal through a stress protocol [27,28]. Unfortunately, experiments in animal models are expensive, both in terms of direct costs and also in terms of experimental effort. Additionally, considerations of ethics have become very demanding regarding the use and restrictions of animal models [29]. These factors suggest a search for valid alternative or parallel approaches, notwithstanding the undeniable fact the traditional paradigm of investigation has greatly advanced science and clinical understanding and will be a mainstay throughout the foreseeable future.

One potential alternative is computational modeling, whose power has increased enormously in recent years, both due to striking advances in computing and the availability of very rich molecular datasets. The core of any computational approach is the representation of a biomedical system through mathematical equations, often in the format of ordinary differential equations (ODEs). Once such a mathematical model is assembled, parameterized and coded in algorithmic software, simulations and other explorations of numerous scenarios are cheap and fast. Although these types of "experiments" must always be followed up with biological or clinical validation studies, they often "weed out" erroneous hypotheses, help us explain and predict an organism's functioning, and guide the design of targeted experiments that advance the field and may eventually lead to novel pharmaceutical interventions.

Employing such a modeling approach, our overall goal in the present study is to deepen our understanding of the interactions within neurotransmitter systems that contribute to the etiology of clinical depression. This goal is pursued through computational simulations with a new mathematical model that elucidates the key components driving the dynamic interactions among the dopaminergic and serotonergic pathways on the one hand and kynurenine metabolism and the role of CORT on the other. The computational analyses focus on chronic stress scenarios and are specifically designed to explain the consequences of changes in these interactions for the onset of MDD.

Results

Conceptual model and dynamic model equations

The model is conceptually based on the pathway system in Fig 1. The translation of this diagram into a so-called Generalized Mass Action (GMA) model is technically straightforward [30,31] and yields the set of equations shown in S1 Supplement (see also Section Methods). The relative steady-state values for each dependent variable and the values for the independent variables are shown in the Tables A and B in S3 Supplement, respectively.
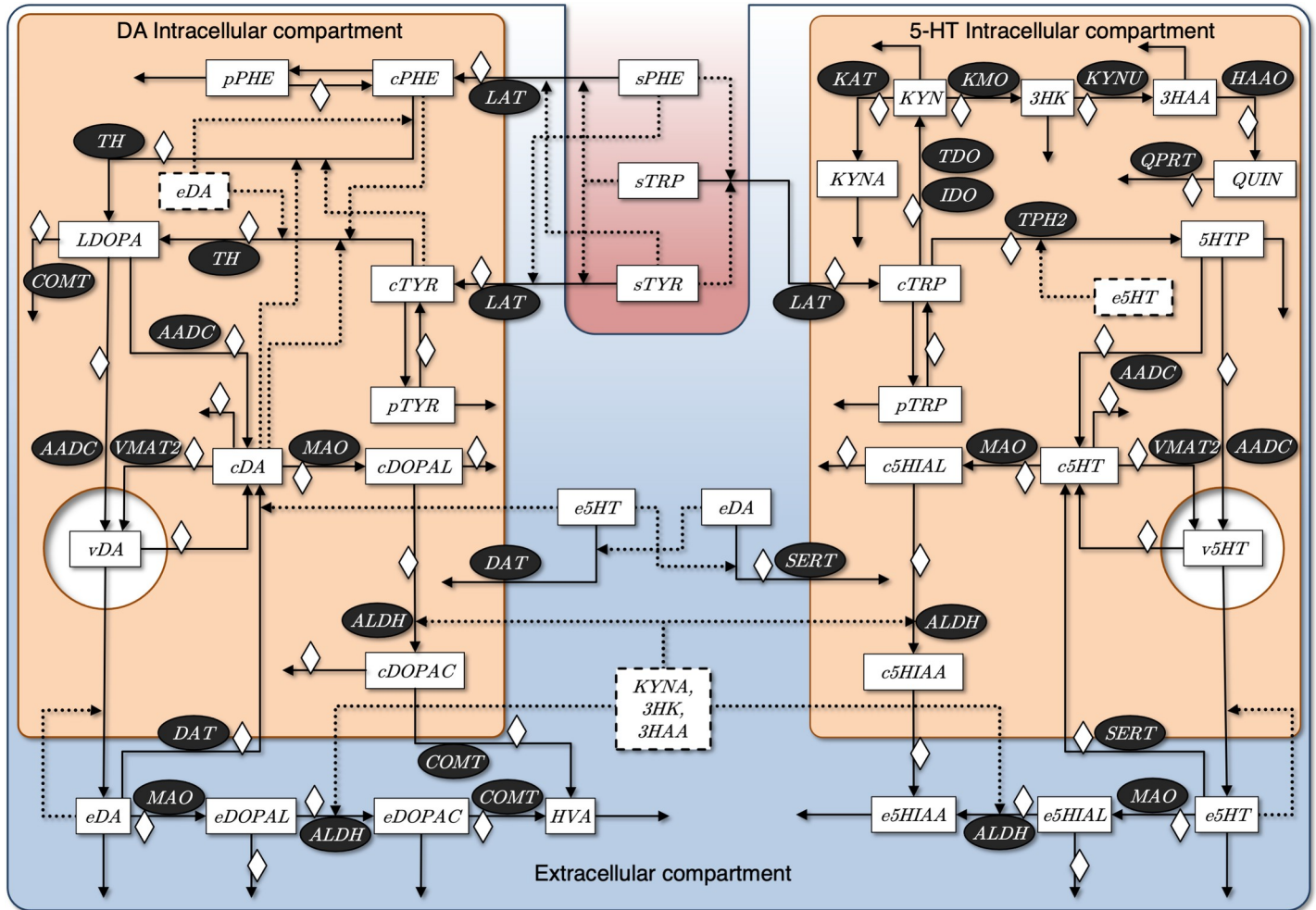
Fig 1. Conceptual, simplified model of pathways associated with MDD and their interactions in the presynaptic DA and 5-HT terminals. The model accounts for separate cytosolic and vesicular compartments in the two terminals, which share the same extracellular space. The latter is an important "collective" location for processes that take place outside the neurons, in particular, in the synaptic cleft or in glial cells. Metabolites are represented with white boxes and participating enzymes with black ellipses. Metabolites in dashed boxes are important but not necessarily located in the compartment where they are represented. Prefixes *s, c, v, e,* and *p* refer to metabolites in the serum, cytosol, vesicles, extracellular space and pool of proteins, respectively. Cortisol/corticosterone (CORT) is represented by a white diamond. Serum tyrosine, phenylalanine, tryptophan, enzymes and CORT are independent variables that remain constant during a given experiment. The strongest inhibitory effects are represented with dotted lines. Abbreviations: 3-HAA, 3-hydroxyanthranilic acid; 3-HK, 3-hydroxykynurenine; 5-HIAA, 5-hydroxyindoleacetic acid; 5-HIAL, 5-hydroxyindoleacetaldehyde; 5-HT, 5-hydroxytryptamine or serotonin; 5-HTP, 5-hydroxytryptophan; AADC, l-amino acid decarboxylase; ALDH, aldehyde dehydrogenase; COMT, catechol O-methyltransferase; DA, dopamine; DAT, dopamine transporter; DOPAC, 3,4-dihydroxyphenylacetic acid; DOPAL, 3,4-dihydroxyphenylacetaldehyde; HAAO, 3-hydroxyanthranilate 3,4-dioxygenase; HVA, homovanillic acid; IDO, indoleamine 2,3-dioxygenase; KAT, kynurenine aminotransferase; KMO, kynurenine 3-monooxygenase; KP, kynurenine pathway; KYN, kynurenine; KYNA, kynurenic acid; KYNU, kynureninase; LAT, L-type amino acid transporter; L-DOPA, l-3,4-hydroxyphenylalanine; MAO, monoamine oxidase; PHE, phenylalanine; QPRT, quinolinate phosphoribosyltransferase; QUIN, quinolinic acid; SERT, serotonin transporter; TDO, tryptophan-2,3-dioxygenase; TH, tyrosine hydroxylase; TPH2, tryptophan hydroxylase 2; TRP, tryptophan; TYR, tyrosine; VMAT2, vesicular monoamine transporter 2.

Sensitivity analysis

Sensitivity analysis quantifies how numerical changes in model settings affect the dependent variables, which here are metabolite concentrations. Specifically, we analyze a special set of sensitivities, called log gains, that quantify relative changes in the steady-state values of metabolites in response to 10% changes in any of the independent variables. We performed this comprehensive gain analysis for two reasons. First, moderate gains, with plus or minus signs, are generally associated with a valid model, because under normal, healthy conditions, most

dependent variables are not expected to vary enormously in response to a small change in any of the independent variables. Thus, the magnitudes of such responses are of interest in systems analysis, and small magnitudes typically indicate model robustness, whereas large magnitudes are often a cause for concern. Expressed differently, the magnitudes provide a qualitative measure of the reliability of the model. Indeed, all gains in our model are reasonable, as it can be seen in S4 Supplement, which demonstrates the mathematical consistence of the model.

Data-based model validation

Simulation experiments were performed to compare the model output with experimental data and clinical findings reported in the literature. Specifically, we considered perturbations in the key enzymes and transporters, namely monoamine oxidase (MAO), catechol O-methyltransferase (COMT), dopamine transporter (DAT), serotonine transporter (SERT), and tryptophan hydroxylase 2 (TPH2). We also investigated their inhibition, as well as the doubling of the activity of the vesicular monoamine transporter 2 (VMAT2), which is a driver of neurotransmitter dynamics [30,32,33]. For these simulations, the model was set to the control state, *i.e.*, the kinetic orders for the variable CORT were set to zero to represent baseline levels of glucocorticoids (absence of chronic stress). The main results are summarized in Table 1.

The results in Table 1 demonstrate that the model with its parameterization aligns quite well with biological and clinical observations. In particular, all predicted model responses, without exception, correctly point in the observed direction of findings reported in the literature. In many cases, the magnitudes are captured semi-quantitatively. For larger deviations,

Table 1. Metabolite changes predicted by the model in comparison to corresponding values found in the literature. Abbreviations: 5-HT, serotonin; COMT, catechol O-methyltransferase; DA, dopamine; DAT, dopamine transporter; DOPAC, 3,4-dihydroxyphenylacetic acid; HVA, homovanillic acid; MAO, monoamine oxidase; SERT, serotonin transporter; TPH2, tryptophan hydroxylase 2; VMAT2, vesicular monoamine transporter 2.

Experiment	Metabolite	Model	Literature
MAO-A/B[-/-]	Extracellular DA	↑34.4%	↑3.2–11.6% [34]
	Total DA	↑133%	↑12 − 200% [35,36]
	Extracellular DOPAC	↓88%	↓21–78.1% [34]
	Total DOPAC	↓70.7%	↓17 − 62% [36]
	HVA	↓64.1%	↓30 − 48% [36]
	Total 5-HT	↑34.8%	↑209–700% [35,37]
	Total 5-HIAA	↓97%	↓81.8% [38]
COMT^{-/-}	Extracellular DA	↑10.6%	↑8.6–52% [39,40]
	Total DA	↑39.1%	↑40% [41]
	Extracellular DOPAC	↑646%	↑233–628% [39,40]
	Total DOPAC	↑318%	↑387% [39]
	HVA	↓67%	↓100% [39]
DAT^{-/-}	Extracellular DA	↑119%	↑393% [42]
	Total DA	↓71.5%	↓96% [42]
	Total 5-HT	↑3.7%	↑3.1% [37]
SERT^{-/-}	Extracellular 5-HT	↑369%	↑450–900% [43–45]
	Total 5-HT	↓27.4%	↓53.8–76.7% [44,45]
	Total 5-HIAA	↓74.8%	↓44.4–55.6% [44,45]
TPH2^{+/-}	Extracellular 5-HT	↓15%	↓66.2% [46]
	Total 5-HT	↓33.7%	↓78.5% [46]
	Total 5-HIAA	↓54.3%	↓72.2% [46]
Two-fold VMAT2	Extracellular DA	↑26.3%	↑44% [32]
	Total DA	↑102%	↑21% [32]

https://doi.org/10.1371/journal.pcbi.1008956.t001

the magnitudes are not always captured accurately, which is to be expected from a model that is naturally based on approximations and simplifications. Overall, hallmark perturbations such as SERT inhibition, which is widely used to increase extracellular 5-HT, validate our model, at least in a semi-quantitative manner.

Model experiments with elevated CORT

To simulate chronic stress in our experiments, we increased the level of CORT to 150% of its baseline value and computed the new steady-state metabolite concentrations in comparison to their steady-state levels when CORT is operating under physiological conditions (baseline of 100%). Fig 2 displays a profile of the most interesting model components for the case of chronic stress. We also included in this analysis the neurotoxic ratios defined by the relationship between quinilinic acid (QUIN) and kynurenic acid (KYNA), and between KYNA and 3-hydroxykynurenine (3-HK).

The results in Fig 2 are very interesting. First, Badawy & Morgan [26] observed in liver that KYNA, 3-HK and 3-hydroxyanthranilic acid (3-HAA) inhibit the activity of aldehyde dehydrogenase (ALDH), and one might reasonably expect the same to be true in the brain; the corresponding model results are displayed in Table 2. According to Fig 2, CORT stress increases the levels of KYNA (↑44%), 3-HK (↑81%) and 3-HAA (↑112%), which in the model leads to inhibition of the activity of ALDH. This model prediction is supported by the elevated levels of the cytosolic aldehydes 5-hydroxyindoleacetaldehyde (5-HIAL) (↑160%) and 3,4-dihydroxyphenylacetaldehyde (DOPAL) (↑29%), which are substrates of ALDH. Second, the model with settings for stress conditions predicts significant increases in KYN (↑61%) and in the neurotoxic ratio QUIN/KYNA (↑65%), as well as a decrease in the ratio KYNA/3-HK (↓21%).

Finally, the model allows us to test interventions that could become potential therapeutic strategies, such as: increase VMAT2 activity (Fig 3A); inhibit SERT (Fig 3B); inhibit kynurenine 3-monooxygenase (KMO) (Fig 3C); and combine inhibition of SERT and KMO (Fig 3D). In addition, Table 2 summarizes the effects of the various simulated "treatments" on key metabolite levels under high levels of CORT. The differences between treated and untreated cases in Table 2 are used in the following discussion.
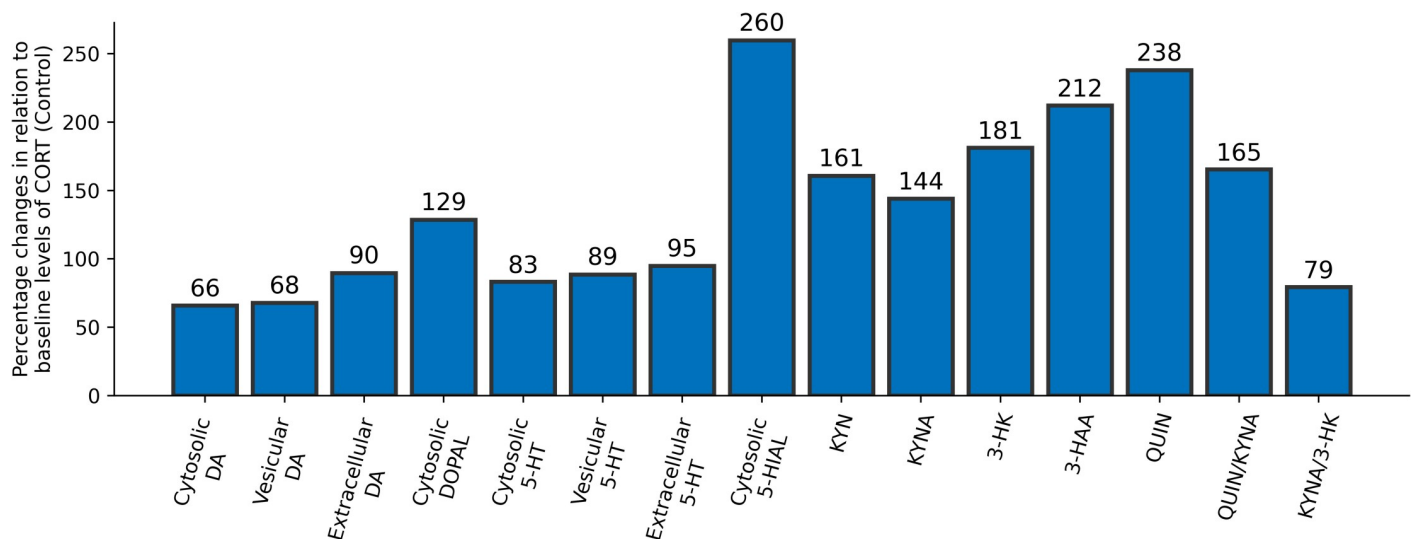

Fig 2. New steady-state values of dependent variables in response to a 50% increase in CORT. The percent changes were calculated in comparison to the corresponding values under control conditions (CORT at baseline of 100%). Also shown are the ratios QUIN/KYNA and KYNA/3-HK, which reflect the balance between levels of key metabolites.

https://doi.org/10.1371/journal.pcbi.1008956.g002

Table 2. Summary of general assumptions made during model design.

Assumption	Comments
The blood-brain barrier (BBB) has just one layer.	The BBB is mainly composed of endothelial cells, which are connected to each other through tight junctions. The only way to cross the BBB is through specific transporters located in the luminal and abluminal membranes (double layer) of the brain capillary endothelia [86,87]. For simplicity, a single layer and one generic type of transporter were considered.
The BBB is the only way for molecules to reach the brain cells.	Since the surface of BBB is more than 1,000 times that of the choroid plexus [88], the BBB area is taken as the exclusive means for a given molecule to access the brain [89].
The L-type amino acid transporter (LAT) is the only one in along the BBB.	Large neutral amino acids (LNAAs), such as tyrosine (TYR), phenylalanine (PHE) and tryptophan (TRP) compete for the same type of transporter, called the L-type amino acid transporter (LAT) [90]. Although different subfamilies of LAT transporters are known, LAT-1 is here assumed to be the sole bidirectional, sodium-independent, high-affinity obligatory exchanger that works for facilitated diffusion.
Only TYR, PHE and TRP cross LAT-1.	In reality, LAT-1 is used not only for passage of TYR, PHE and TRP, but also for transporting brain- chained amino acids (BCAA) [91]. This fact appears to be of secondary importance, and the inhibitory competition of these BCAA in the uptake of TYR, PHE and TRP was not taken into account.
The transport of LNAA occurs directly from the blood serum to the neuronal cytosolic space.	In actuality, LNAAs reach the brain neurons by entering an astrocyte or moving through the extracellular space to a neuron. In the model, these steps are simplified to a single transport step across the BBB through LAT-1, directly to the neuron, as was proposed in the literature [48,49].
Only TYR and PHE affect the dopaminergic pathway, while TRP acts only in the serotonergic pathway.	Uptake of TYR, PHE and TRP can lead into both dopaminergic and serotonergic neurons through intersection points in the two pathways [92–94]. For simplicity, we assume that only TYR and PHE enter dopaminergic neurons, while TRP only enters serotonergic neurons.
The intracellular volume of a nerve terminal is $V_i = 1.13 \times 10^{-10}\ \mu l$	Volume estimates are necessary for scaling the results. Direct information is unavailable and the estimates are quite coarse, but appear to be sufficient, as the relative sizes to each other are more important. If such a terminal is taken as a single synaptosome and approximated by a sphere with radius $R_i = 300\ nm$, the corresponding intracellular volume is $V_i = 1.13 \times 10^{-10}\ \mu l$ (notice that this is not the cytosolic volume, but the cell volume as a whole).
The intracellular vesicular volume in a nerve terminal is $V_v = 6.7 \times 10^{-12}\ \mu l$	Each terminal contains approximately 200–500 vesicles of approximately 40 nm in diameter [95–97]. Taking every vesicle as a sphere with radius $R_v = 20\ nm$ and multiplying its volume by 200 results in a total vesicular volume $V_v = 6.7 \times 10^{-12}\ \mu l$.
The cytosolic volume in a nerve terminal is $V_c = 1.06 \times 10^{-10}\ \mu l$	Taking V_i and V_v as above described, the cytosolic volume is, consequently, $V_c = V_i - V_v = 1.06 \times 10^{-10}\ \mu l$.
The extracellular volume surrounding one nerve terminal is $V_e = 1.78 \times 10^{-11}\ \mu l$	The extracellular space surrounding the nerve terminal is assumed to be a 15 nm-thick layer [98]. With the above settings, the extracellular space in the immediate vicinity of a terminal, if expressed as a sphere, has the volume $V_e = 1.78 \times 10^{-11}\ \mu l$. Considering that there are two terminals, the total shared extracellular volume is $2V_e$.

(*Continued*)

Table 2. (Continued)

Assumption	Comments
Conversion factor from grams of tissue to volume of water: $f_c = 0.7\ ml/g$	Units of metabolite concentrations and enzyme kinetic parameters must be consistent to calculate the kinetic orders for power-law approximation. Fluxes and affinities are usually given in molar concentration per unit of time ($mol/l/h$) and molar concentration (mol/l), respectively, or in fractions of these units. We used a conversion factor $f_c = 0.7\ ml/g$ to switch between mol/g and mol/l [99,100], when necessary.
Every component in the model is assumed to be homogeneously spread throughout the same compartment.	The consideration of spatial heterogeneity would increase the complexity of the model manyfold.
The CORT concentration is assumed to vary proportionally and homogeneously regardless of the compartment.	Since CORT if a lipophilic molecule with low weight, it can cross the BBB by diffusion and quickly disperse toward the concentration equilibrium [101]. It has been shown that changes in CORT levels are easily detected in saliva and urine and that these measurements correlate well with free serum CORT concentrations [102,103]. Thus, absolute values and changes for CORT concentrations taken from saliva, urine or serum are assumed to represent alterations inside the brain cells [104].
Kynurenine metabolites are assumed to vary proportionally and homogeneously regardless of the compartment.	Information regarding KYN-associated metabolite concentrations in dopaminergic and serotonergic neurons is scarce. However, it is fair to assume that these levels are in the nanomolar (nm) range within tissues and in the extracellular space. The concentrations of the KYN metabolites of interest are considered uniformly distributed over brain cells and compartments.
Transcriptional and post- translational regulation mechanisms are not considered, so that protein expression is assumed to be directly proportional to gene expression.	Experiments with homozygote and heterozygote mutants in animals do not necessarily result in a 100% and a 50% reduction in protein expression or activity, respectively. However, for simplicity, transcriptional and post-translational mechanisms are ignored, and it is assumed that there is a linear correlation between gene and protein expression [105,106].
Proteins are represented as a fraction of the total amount of protein content in the control situation.	All variables of a mathematical model that in a simulation do not change over time can be explicitly represented as independent variables and defined as constants. Here, this is the case for the proteins involved in enzymatic reactions.
Enzyme concentrations vary to the same degree regardless of the compartment in which they are active.	Although the enzyme concentrations may vary according to the compartment where they are located, it is assumed that their levels change proportionally everywhere, according to the protocol of the experiment, in which proteins are independent variables with values set before each simulation.
Chronic stress is positively correlated to inflammation.	A large body of research has demonstrated an association between social stressors and inflammation. These studies provide evidence of the correlation among stress, depression and the immune system at the levels of proteins, signaling processes and the genome [107].
Chronic stress is positively correlated to cortisolemia.	Chronic stress leads to a reduction in the negative feedback affecting the HPA axis, thereby elevating the levels of CORT over time. In addition, immune cells become less sensitive to the anti-inflammatory effects of CORT, which leads to the so-called "glucocorticoid insensitivity" [108].
Aspects of comorbidities accompanying depression were not taken into account.	MDD usually manifests with other disorders, such as anxiety and post-traumatic stress disorder [109], whereas our model is based on findings concerning depressed patients and animal models of depression.

(Continued)

Table 2. (Continued)

Assumption	Comments
Neuronal firing was not taken into account.	Although neuronal firing activity plays a key role in neurotransmission and, consequently, in the levels of metabolites, our model focuses only on the biochemical reactions that regulate the monoamine systems.

https://doi.org/10.1371/journal.pcbi.1008956.t002

A two-fold increase in the activity of VMAT2 elevates the levels of monoamines (vesicular, extracellular and total), which is desirable. However, the level of the cytosolic 5-HIAL remains too high (Fig 3A), with a difference of only ↓10% in comparison to the untreated situation. Also, no significant changes in the levels of kynurenine metabolites were observed, especially in 3-HK and QUIN, which are neurotoxic.

By contrast, the inhibition of SERT leads to a strong increase in extracellular 5-HT (↑360%) and a decrease in the level of the cytosolic aldehyde 5-HIAL (↓93%), but not the levels of cytosolic DOPAL, which is actually slightly increased (↑6%) in comparison to the untreated system (Fig 3B). No relevant changes were observed in the kynurenine metabolites.

Since 3-HK is also neurotoxic and serves as an early precursor for the production of QUIN, it is important to find the right balance between the levels of KYNA, 3-HK and QUIN. Along these lines, a simulation with our model demonstrates that inhibition of KMO by 50% reduces the increase in the ratio of QUIN/KYNA (↓31%) and increases KYNA/3-HK (↑86%). Moreover, this strategy causes a small decrease in the level of cytosolic DOPAL (↓8%). Unfortunately, the level of the cytosolic aldehyde 5-HIAL remains high (Fig 3C), even with a decrease of 16%. Notice also that there is no increase in the levels of the extracellular monoamines.

According to the model, the combined inhibition of SERT and KMO not only increases the levels of extracellular 5-HT (↑353%), but also of extracellular DA (↑30%) in comparison to the untreated CORT state (Fig 3D). Although the change in cytosolic DOPAL is relatively low (↓3%), cytosolic 5-HIAL declined 94%. Besides decreasing the levels of aldehydes, this intervention also decreases the neurotoxic ratio, QUIN/KYNA (↓31%), and increases the KYNA/3-HK ratio (↑86%).

Discussion

We have developed and parameterized a dynamic model to test the impact of elevated cortisol/corticosterone levels and their consequences on serotonin, dopamine and kynurenine pathways, which are known to be associated with the etiology of MDD. Previous models have investigated the interplay of dopaminergic and serotonergic pathways in different contexts, such as the influence of firing and the roles of autoreceptors [47–50]. However, to the best of our knowledge, this is the first mathematical model integrating all pertinent biochemical pathways into a model of depression. Altering parameters in key components of these metabolic pathways generated model predictions that were confirmed by available experimental data; these predictions are therefore acceptable for testing in increased glucocorticoid conditions. High glucocorticoid conditions lead to a detrimental decrease in serotonin production, which is typical of MDD, and were damaging to the activation of the KP. Most importantly, our model predicts significant increases in the cytosolic aldehydes DOPAL and 5-HIAL, in addition to imbalances in the QUIN/KYNA and KYNA/3-HK ratios, which are directly related to neurotoxicity. Therefore, our model suggests the hypothesis that increased levels of DA and 5-HT catabolism, DOPAL and 5HIAL may be important contributors to chronic depression, as they lead to the activation of neurotoxic effects.
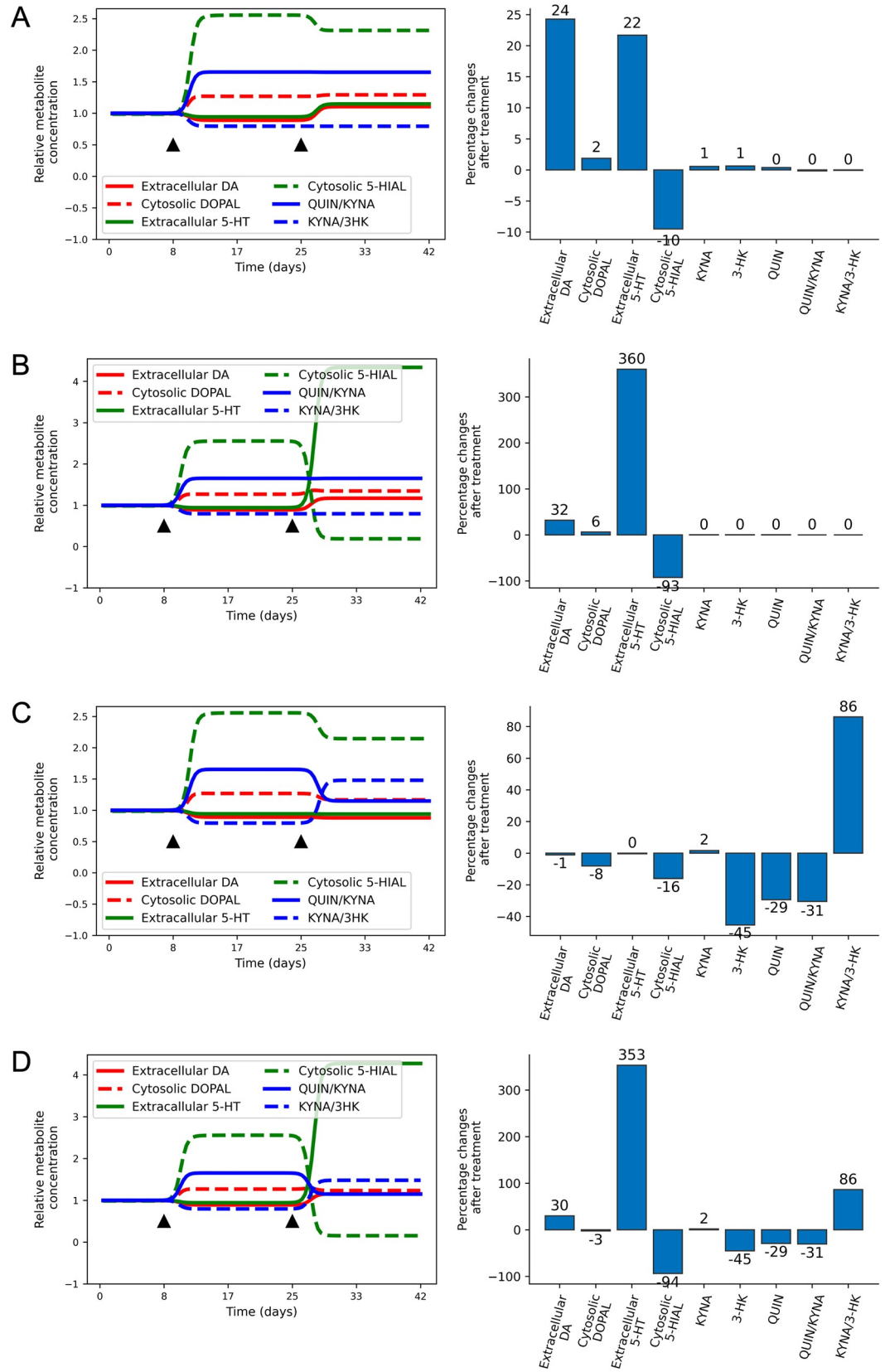
Fig 3. Notable changes in key dependent variables in response to cortisolemia and treatment. (A) Two-fold increase in the activity of VMAT2. (B) 95% Inhibition of the transporter SERT. (C) 50% Inhibition of the activity of enzyme KMO. (D) Combined inhibition of SERT ($\downarrow$95%) and KMO ($\downarrow$50%). Time courses are shown on the left and percent changes after treatment on the right of each panel. CORT is increased by 50% at day 8 and "treatment" starts at day 25 (black triangles).

https://doi.org/10.1371/journal.pcbi.1008956.g003

According to our model, increased levels of CORT are associated with significant increases in the concentrations of KYNA, 3-HK, and 3-HAA. The increased levels of DOPAL and 5-HIAL reflect evidence of an inhibited ALDH, which in turn is connected to an increased activity of MAO, which becomes evident in the decay of the overall levels of monoamines in our simulation. It is known that these aldehydes are extremely reactive and toxic for the neuron, and rodent studies have demonstrated that DOPAL and 5-HIAL lead to the oligomerization of α-synuclein (αS) [51,52]. Interestingly, recent findings indicate increased levels of αS in the serum of patients with MDD [53], as well as increased amounts of αS-DOPAL oligomers that impair the function of synaptic vesicles, induce DA leakage and further reduce neurotransmission [54].

Studies in humans as well as animal models suggest that αS oligomers lead to mitochondrial dysfunction, and this impairment has been shown to be mediated by the innate immune system and is related to the pathophysiology of MDD [55]. More specifically, fusion or fission processes seem to be especially affected by αS, causing mitochondrial fragmentation [56]. Intriguingly, ALDH is a protein associated with mitochondria, which supports the speculation that its impaired function possibly leads to neurotoxicity that often accompanies cortisolemia. This conclusion is in agreement with a recent study showing that chronic stress does not seem to change the expression of ALDH but can damage the signaling pathway involved with the function of this enzyme in the HPC and PFC [57].

Oxidative stress is the initial step of lipid peroxidation. Here, it yields aldehydes that reduce the level of 3,4-dihydroxyphenylacetic acid (DOPAC) and elevate DOPAL to abnormal levels by inhibiting ALDH activity [58,59]. Evidence of pro-inflammatory cytokines triggering oxidative stress have led to the suggestion of the so-called "oxido-neuroinflammation hypothesis" for the pathogenesis of MDD [60]. The increases in aldehydes and in neurotoxic kynurenine metabolites with high levels of corticosteroids shown by our model support this hypothesis.

It is well known that glutamate can induce neurotoxicity and neuronal death through its agonistic activity on the NMDA receptor. Furthermore, depending on its concentration, KYNA can act on the glycine and/or glutamate modulatory binding sites of the NMDA receptor playing a neuroprotective role by inhibiting the NMDA receptor activity. Conversely, several studies have demonstrated that QUIN stimulates the NMDA receptor, acting as its agonist [25,61], and inhibits its uptake by glial cells, which augments the availability of glutamate [62] and neurotoxicity. Our model does not explicitly include astrocytes and their interactions with the monoaminergic systems, but it could be interesting to explore how glial cells might expand insights gained here.

Elevated levels of these neurotoxic metabolites and of circulating CORT have been correlated with a reduction in HPC volume and dendritic atrophy of its nerve terminals, as observed in MDD patients [63–66]. It has specifically been shown that the increased concentration of 3-HK is associated with neuronal apoptosis in the HPC [67] and that excess extracellular glutamate is related to reduction in dendritic growth [68]. In addition, since HPC is known for having the highest glucocorticoid binding activity of any brain structure [69], the hippocampal control over the hypothalamic-pituitary-adrenal axis is mediated by CORT [70]. These findings are consistent with the widely reported neuropsychological deficits due to hippocampal impairments and volume loss that were observed in untreated MDD patients [71–73].

Our results point to the accumulation of 3-HK and toxic imbalance in the ratio QUIN/ KYNA under cortisolemia, besides the increased levels of DOPAL and 5-HIAL. Such dysfunctions are due to changes caused by cortisol in the activity of enzymes in the KP and the monoaminergic system, such as MAO, indoleamine 2,3-dioxygenase (IDO), tryptophan-2,3-dioxygenase (TDO), kynurenine aminotransferase (KAT), and 3-hydroxyanthranilate 3,4-dioxygenase (HAAO). Hence, we propose that all these mechanisms can cause the neuronal death or atrophy in the HPC and PFC as they are observed in depressed patients.

In terms of possible therapeutic targets, our model suggests that overactivating VMAT2 expression twice, a strategy proposed as a therapeutic intervention to re-establish the physiological levels of DA in patients with Parkinson's diseased or bipolar disorder [32], does not seem to be an efficient approach in comparison to the untreated system, at least with regard to higher levels of glucocorticoids. Also, we observed that the levels of aldehydes and kynurenine metabolites did not change to a meaningful degree, therefore maintaining neurotoxicity.

The model was able to mimic the effect of inhibiting SERT, which leads to a consistent increase in extracellular levels of 5-HT and decreased levels of cytosolic 5-HIAL. By using three classes of pharmacological approaches, two of them interacting with norepinephrine, one of them a SSRI, Martín-Hernández et al. (2019) demonstrated an increase in QUIN/ KYNA ratio in the frontal cortex of rats under mild chronic stress and a return to the baseline situation after treatment with antidepressants [74]. However, they found a decrease in the expression of HAAO, although not in all KAT isoforms, which implies that antidepressant treatment can reduce the neurotoxic risk ratio, but at the cost of increasing the levels of KYNA, whose levels are positively correlated to cognitive impairment found in patients with schizophrenia [75]. Moreover, higher levels of 3-HK increase the neuronal vulnerability in patients with Huntington's disease [76]. Since 3-HK is also neurotoxic and is an early precursor in the production of QUIN, it is essential to find a proper balance between the levels of KYNA and 3-HK and QUIN.

Our current model focuses on DA and 5-HT but by and large ignores the roles of other neurotransmitter systems, such as the role of norepinephrine metabolism in MDD [77]. It could therefore be interesting to expand the current model toward an inclusion of this pathway and explore the so-far ill-characterized molecular mechanisms involved in the interactions between the monoamine system, antidepressants and KP. Such an expansion is currently not feasible, due to many gaps in information, but could be intriguing once experimental studies provide additional data.

Although it seems to be intuitive and straightforward to propose a treatment based on the inhibition of IDO to slow down the KP, it has been shown that such an approach is related to pro-carcinogenic side effects [78]. Also, our gain analysis did not identify a significant impact of IDO on 3-HK, 3-HAA and QUIN. Nonetheless, along these lines, we propose the inhibition of KMO as a possible adjuvant intervention. The corresponding simulation with our model demonstrates that inhibition of KMO is able to reduce QUIN/KYNA while increasing KYNA/ 3-HK, which is in agreement with other findings in the literature [79]. Interestingly, it has been shown that some KMO inhibitors are more effective in reducing QUIN and 3-HK in situations of strong immune activity [80]. According to our model, the combined strategy of inhibiting SERT and KMO seems to be promising. Hence, we propose the further exploration of KMO inhibitors, in combination with SERT inhibitors, for controlling the production of neurotoxic kynurenine metabolites that is due to the well-known shift in tryptophan metabolism under chronic stress.

In conclusion, our model is the first to suggest that high corticoids trigger an increase in the levels of neurotoxic aldehydes DOPAL and 5-HIAL, which are directly derived from DA and 5-HT catabolism, and that this increase may contribute to chronic depression. This hypothesis

implies that the interaction between KP and the dopaminergic and serotonergic catabolic pathways might be an important therapeutic target in MDD. The neurotoxic risk ratio QUIN/KYNA is increased when the level of CORT is elevated, probably leading to glutamate excitoxicity by activation of NMDA receptors. This chain of events may be a key component of PFC neuronal atrophy observed in patients with MDD. To counteract these effects, the computational simulations using classical inhibitors for serotonin and kynurenine pathways suggest that a therapeutic strategy combining SERT and KMO inhibitors would be more effective than SERT inihibition alone. More generally, the recognition of the systemic nature of multiple interacting factors that are involved in MDD and lead to prolonged symptoms and possible brain damage is a fundamental step forward in the development of more efficacious therapeutic approaches.

Methods

Pathway structure

The unusual cellular architecture of the PFC includes dopaminergic and serotonergic terminals, even though the cell bodies are located elsewhere. It is therefore reasonable to model the metabolic pathways of dopamine and serotonine-kynurenine in the axon terminals of PFC neurons. The essential details to be included in the model were identified based on literature information, with emphasis on the most relevant metabolic pathways governing DA, 5-HT and KYN within the PFC. Many kinetic features of the reactions were taken from biological databases, such as BRENDA [81], KEGG [82] and MetaCyc [83]. In addition, a few terrific models of some of the pathways of pertinence are available, sometimes in the form of detailed differential equation models. For instance, models are available for the dopamine system [76–77] and the role of levodopa [80], as well as the serotonin pathway [78, 81] and tryptophan and kynurenine metabolism [79]. These models contain much information, some of which we were able to adapt for our purposes. Furthermore, since 5-HT and KYN have tryptophan as a common precursor, KYN metabolism was modeled inside the serotonergic terminal, although most evidence places KYN within the microglia and astrocytes [84,85]. This simplifying assumption seemed reasonable considering that a scientific model is always an abstraction of a complex phenomenon and that we are not concerned about spatial features in this analysis. An overview of the map of reactions and key features within their compartments is shown in Fig 1.

General and specific assumptions

For purposes of unit conversions, formulation and simulations, some quantitative and qualitative assumptions were made in order to facilitate the understanding of the processes and to render the chemical and physical quantities coherent. General assumptions and their biological rationale are summarized in Table 2.

A few additional assumptions are particular to each pathway, depending on the specifics of the metabolites involved in the reactions and the compartments where these reactions take place. The central assumptions and inferences taken from the literature regarding the dopaminergic and the serotonergic-kynurenine pathways are presented in Table 3. Concentration values for dependent variables at the steady state are listed in Table A in S3 Supplement, while explanations of other values are presented in the following subsections.

One additional assumption made in this work is important and should be discussed in some detail. Namely, some pro-inflammatory cytokines enhance the activity of the enzyme IDO, when high levels of CORT stimulate TDO [133,134], thereby shifting tryptophan from the biosynthesis of 5-HT to the production of kynurenine [135]. Also, it has been shown that

Table 3. Summary of the specific assumptions used during model design.

Assumption	Comments
TYR, PHE and TRP inhibit each other.	Since these LNAA compete for the transport through the BBB, they reduce their competitors' net fluxes through LAT-1.
TYR and PHE have just two fates: protein synthesis or synthesis of L-DOPA.	About 90% of the TYR and PHE are used for protein synthesis and 10% for the synthesis of L-DOPA [110]. Furthermore, 90% of the production of LDOPA uses TYR as substrate, since TYR is the preferred substrate of TH.
It is assumed that about 80% of L-DOPA is committed to the synthesis of DA and the remaining 20% is methylated by COMT.	This assumption is reasonable because the majority of L-DOPA is decarboxylated to DA.
At steady state, the concentration of L-DOPA is 10% of the level of cytosolic DA.	Exact proportions are unknown, but similar assumptions were made for other models in the literature [33,48].
Vesicular DA and 5-HT correspond to 98% of the intracellular DA and 5-HT, while the remaining 2% is in the cytosol.	It is generally assumed, and implemented in other models, that most of the intracellular DA is located in the vesicles of dopaminergic neurons [33,48]. The same assumption is made here for serotonergic neurons.
Homovanillic acid (HVA) is considered to exist only in the extracellular space.	The proposed model does not include astrocytes and other glial cells that are involved with the dynamics of HVA. However, COMT is active in the DAergic neurons, so that HVA can also be directly influenced by cytosolic DOPAC.
TRP is assumed to have only three fates: protein synthesis, synthesis of 5- HTP or kynurenine.	It is assumed that about 10% of TRP is used to protein synthesis, whereas 35% is committed to the synthesis of 5-HTP and the remaining 55% is used in the synthesis of kynurenine [79].
It is assumed that about 80% of 5-HTP are committed toward the synthesis of serotonin.	Although 5-HTP plays several peripheral roles, the vast majority is used for the biosynthesis of 5-HT [111].
At the steady state, the concentration of 5-HTP is 10% of the cytosolic serotonin.	A similar assumption is made for DA and L-DOPA.
$eDA/e5HT = 1$	According to the literature, the ratio of $eDA/e5HT$ is between 0.71 and 2, with a tendency toward the lower level [112–115].
$iDA/i5HT = 0.5$	According to the literature, $0.5 < iDA/i5HT < 0.8$, with a tendency toward the lower level [27,116–118].
$i5HT/e5HT = 850$	This value was taken from Adell *et al.* [119].
$e5HIAA/e5HT = 800$	The extracellular concentration of 5-HIAA is much higher than the extracellular concentration of 5-HT [120].
$i5HIAA/e5HIAA = 0.5$	This value was taken from Adell *et al.* [119]. Note that i5HIAA is the tissue concentration of 5-HIAA and had to be converted to cytosolic concentration.
$iDOPAC/eDOPAC = 0.5$	A similar assumption was made for the serotonergic metabolites, intra- and extracellular 5-HIAA. Note, again, that $iDOPAC$ is the tissue concentration of DOPAC and had to be converted to cytosolic concentration, since DOPAC is not present in the vesicle compartment.
$cDOPAL/cDOPAC = 200$	DOPAL has been quantified as the precursor aldehyde of DOPAC in the *substantia nigra* of human brains [121]. We adopted the same ratio for the extracellular compartment ($eDOPAL/eDOPAC = 200$).
Cytosolic DA and 5-HT inhibit their own synthesis.	DA inhibits its own synthesis by competing with the cofactor tetrahydrobiopterin (BH4) for the binding site of the enzyme TH [122,123]. We assumed that 5-HT inhibits its own synthesis by means of a similar competing mechanism.
D_2 is the only auto-receptor whose activity was taken into account; extracellular DA modulates TH activity through D_2.	No other receptors that modulate DA synthesis and release were taken into account, since our study focuses on the presynaptic dopaminergic nerve terminal, where D_2 is most prevalent.

(*Continued*)

Table 3. (Continued)

Assumption	Comments
5-HT$_{1B}$ is the only autoreceptor whose activity was taken into account; extracellular 5-HT modulates TPH2 activity through 5-HT$_{1B}$.	No other receptors that modulate 5-HT synthesis and release were taken into account, since our work focuses on the presynaptic serotonergic nerve terminal, where 5-HT$_{1B}$ is most prevalent.
Extracellular DA competes with extracellular 5-HT for SERT	Although all biogenic monoamine transporters are promiscuous, only the competition of DA for SERT was considered, since the affinity of 5-HT for DAT is much lower than DA for SERT [124–126].
TPH2, AADC and VMAT2 have a functional and physical coupling similar to TH, AADC and VMAT2	It has been shown that TH, AADC and VMAT2 have a functional and physicial coupling, so that DA is directly transported into vesicles as soon as it is synthetized [127,128]. We assume that TPH2, AADC and VMAT2 behave in the same way.
KYNA, 3-HK and 3-HAA inhibit the activity of ALDH in the brain.	Even at low concentrations, these kynurenine metabolites can reduce the ALDH activity by 40% or more in the liver [26]. Although ALDH is not the only enzyme involved in the catalysis of DOPAL and 5-HIAL, these aldehydes are mainly oxidized by ALDH [129].
IDO-TDO, MAO, KAT, and HAAO activities are increased under chronic stress.	A substantial body of research supports these assumptions [74,130–132].

the expression of TPH2 is inhibited by methylation in rat brains under stress [136]. Taken together, these observations imply that during an inflammatory response and increased levels of CORT due to chronic stress, not only are the levels of tryptophan available for 5-HT synthesis diminished, but there is also a genetic regulatory mechanism that decreases the expression of the rate- limiting enzyme TPH2. Although cytokines are not necessarily acting simultaneously, since their levels change over time [137], it was assumed for simplicity that, under chronic stress, the levels of CORT and the levels of proinflammatory cytokines are positively correlated [8,107,108]. To implement this assumption, the variable CORT acts directly on the activity of TDO and indirectly represents the influence of cytokines on the activity of IDO and TPH2, thereby shifting tryptophan from 5-HT to KYN synthesis.

Modeling framework

The choice of the best possible modeling framework is a challenging task, and a lot has been written about it (e.g., [31,138]). Biochemical Systems Theory (BST; [139,140]) was chosen here as the modeling framework, because it is arguably the least biased dynamic approach and requires very few assumptions (*e.g.*, [31]). It is furthermore rigorously based on Taylor's approximation theory of numerical analysis [30,141,142]. Other advantages of power-law models in BST over traditional models include the following.

1. Traditional representations, such as Michaelis-Menten functions, suffer from the well-known problem that they are approximations of mass-action kinetics, which in turn assume operation in a well-mixed, homogeneous medium (see [143]), which of course is not the case in living cells. Thus, the foundation of these wide-spread rate laws is not really present *in vivo*. It may be sufficient, but that is unknown and may differ from case to case. The situation is particularly dire in crowded environments as they exist in living cells [144–146].

2. BRENDA [81] and other databases [82,83] contain ample kinetic information, but the true K_M (let alone V_{max}) values for a specific situation like ours (*i.e.*, cell terminals in a specific brain section, possibly diseased) are very rarely known. The situation is worse for inhibition

and other modulator constants. Furthermore, to formulate a traditional model, the type of mechanism for every inhibition or activation signal needs to be known *a priori*, and if it happens to be allosteric, it is unclear how to represent it mechanistically.

3. Power-law functions may at first appear to be unnecessarily complex and require some getting used to. However, they offer tremendous advantages. First, it is an automatic process to convert a pathway diagram into symbolic power-law equations (*e.g.*, [31]). Namely, every process in every differential equation is represented with a product of power-law terms consisting of a non-negative rate constant and of every variable affecting the process, raised to a real-valued power. Second, in contrast to traditional functions, this representation is mathematically guaranteed (by Taylor's theory of numerical analysis) to be correct close to the normal operating point of the cell or organism if the parameter values are chosen correctly. Third, power-laws contain fewer (or at most as many) parameters than most traditional functions: There is one kinetic order per variable affecting a given process and one rate constants. Compare this parsimony with the traditional rate law of a bi-substrate-bi-product reaction with inhibition, which can demand a dozen or more parameter values [147]. Fourth, the kinetic orders in power-law models almost always have values within small ranges (Chapter 5 of [30]) which makes it easy to assign default values if true values are unknown. These default values allow the modeler at least to get started. Sensitivity analysis subsequently shows how important the value of this kinetic order is.

4. Careful side-by-side comparisons of large metabolic models, represented either with traditional functions or with power-laws have demonstrated very little difference in results (*e.g.*, [148–150]), except for crowded media, where power-laws are clearly superior [144–146].

Of course, the power-law formulation is no panacea and has its germane disadvantages. First, a single term does not model saturation, although steady states are represented well by the equations. Second, the model is by its nature an approximation and usually becomes less accurate as simulations deviate far from a chosen operating point, such as the normal steady state.

BST offers several variants [151], among which we decided for the GMA format, because it reflects the stoichiometric relationships within a metabolic pathway system most intuitively. Specifically, all GMA equations have the following form [31,147]:

$$\frac{dX_i}{dt} = \dot{X}_i = \sum_j \pm \gamma_{ij} \cdot \prod_k X_k^{f_{ijk}} \tag{1}$$

Here, the change of each dependent variable *i* over time (dX_i/dt) is described as a sum or difference of *j* power-law terms, each of which is composed of a positive rate constant γ_{ij} and of *k* variables that directly affect the particular process. Each equation may have different numbers of terms and each power-law may have different variables, so that both indices, *j* and *k*, typically vary throughout the system of ODEs. Each variable X_i is raised to a power f_{ijk}, called a kinetic order, which are usually in the range of -1 (miminum inhibitory influence) and 1 (maximum activating influence). If a variable is raised to the power $f_{ijk} = 0$ the resulting power-law term is 1, and the variable does not affect the term. Like, dependent variables, which may change over time according to the dynamics of the system and have their own differential equation, independent variables, such as enzyme concentrations, are included in each pertinent term. These variables typically do not change during a given computational experiment or simulation, and they are under the control of the experimenter [33,152,153]. Although the notation in Eq 1 looks restrictive, it is worth noting that the overall model structure is enormously rich and can represent any nonlinearities [151].

The equations of our model can be found in S1 Supplement.

Once the structure of the pathway system is known, it is immediately possible to translate this structure with all details into symbolic power-law equations. This "automatic" formulation is a tremendous advantage over other approaches, and the remaining challenge is the task of determining numerical values of all parameters from data or literature information. An intriguing, multi-decade experience is the fact that BST models are so robust that even relatively substantial variations in kinetic orders, of maybe 30%, usually do not compromise the meaning of a model response, as long as the structure of the biological system is correctly represented and all the relevant connections and metabolites are taken into account [33].

Parameter identification

While the design of a symbolic BST model is straightforward, the estimation of parameter values is a challenge, as it is for all other model types. Where available, quantitative and qualitative experimental or clinical information was converted into parameter values, with methods that have been demonstrated many times (*e.g.*, [30,31,154]). Information embedded in other types of models was directly converted with purely mathematical means [148–150]. Nonetheless, as is to be expected, not all pertinent information was available, which required us to use default values (see [30,33]) and computational adaptations so that qualitative results matched observations.

Specifically, the model was fit in two phases: the "control state" and the "CORT state". The control state was defined as a vector of model variables for the value of CORT at its baseline. In a mammalian model under physiological conditions, some of the variables refer to the basal levels of circulating corticosterone. This corticosterone oscillates during the day, but it is generally assumed that the level does not significantly affect the steady states of neurotransmitter metabolites. For calibrating the model at the control state, the variable CORT was fixed as a constant, and data taken from animal experiments found in the literature were used to adjust the default values of kinetic orders in some reactions to fit additional experimental data (see Table C in S2 Supplement).

It is important to note that the minimal effect of corticosterone on neurotransmitters under normal conditions does not hold for chronic stress situations. Thus, in the second phase of model calibration, the CORT state was analyzed. Specifically, to estimate the parameter values related to corticosterone, all kinetic orders determined for the control state were fixed and only the kinetic orders for CORT (increased by a factor greater than 1, *i.e.*, > 100%) were adjusted based on data from experiments on chronic stress in animal models (see Table C in S2 Supplement). Finally, the rate constants were calculated for the final set of power-law equations according to the methodology described in [30] and based on the flux partitioning ratios taken from other models in the literature [33,47–50,79,155].

In both situations, an additional constrained optimization was performed to achieve an ensenmble of well-fitting models. Initially, several sets of random kinetic orders were generated using Latin Hypercube Sampling (LHS) of 100 *d*-size [156], where *d* is the number of parameters to be optimized. Every set of the Latin hypercube values was tested and the residual mean squared error (MSE) for each parameter combination was calculated. At the end, 5% of the results with the lowest MSE were selected as initial values for a follow-up local search optimization, using the Nelder-Mead algorithm [157]. Among the optimized sets of parameters, a value was chosen that appeared to be clinically most suitable. The equations of our model can be found in S1 Supplement and the final sets of kinetic orders and rate constants are shown in Tables A and B in S2 Supplement, respectively.

Model validation

Two approaches were used to assess the reasonableness of the model: one strictly mathematical, the other based on data.

The first approach to validating the parameterized model was a typical sensitivity analysis, which allowed us to judge the adequacy and robustness of the mathematical formulation of the system (for different variants of this type of analysis, see [30]). Specifically, we focused on "logarithmic (log) gains", each of which quantifies the relative (percent) change in the steady-state concentration of a metabolite (dependent variable) in response to a small-percent change in an independent variable, such as an enzyme activity or hormone level. We performed this analysis for 1% and 10% variations.

The second approach used the comparison of predicted results against data not used to calibrate the model. Specifically, if experimental data are too scarce to allow rigorous parameter estimation and model validation, other strategies must be found to validate the model. In our case, for example, the complexity of the brain is so enormous that there is no guarantee that neuronal metabolism in the *substantia nigra* or the striatum is the same, or even similar, in the PFC [158]. In particular, there are only a few datasets reporting metabolic measurements in the PFC of animals under chronic stress, and other information to verify the behavior of the model variables does not exist. Thus, the best that can be done is a qualitative or semi-quantitative comparison between the results obtained from our model in specific scenarios and the corresponding results from experiments (*in situ*, *ex vivo*, *in vitro* or computational) that are in some sense similar although not exactly equivalent.

Simulation framework

The parameterized model was implemented in the free platform Python, version 3.8, and run on a MacBook, dual-core processor Intel Core i7, 1.7 GHz, 8 GB RAM, and 64 bits of operating system.

Supporting information

S1 Supplement. Model equations.
(DOCX)

S2 Supplement. Results of the parameter estimation, including literature sources.
(DOCX)

S3 Supplement. Physiological values of dependent and independent variables.
(DOCX)

S4 Supplement. Sensitivity analysis.
(DOCX)

Acknowledgments

Author Contributions

Conceptualization: Felipe Dalvi-Garcia, Luis L. Fonseca, Cecilia Hedin-Pereira, Eberhard O. Voit.

Data curation: Felipe Dalvi-Garcia.

Formal analysis: Felipe Dalvi-Garcia.

Funding acquisition: Ana Tereza R. Vasconcelos, Cecilia Hedin-Pereira, Eberhard O. Voit.

Investigation: Felipe Dalvi-Garcia.

Methodology: Felipe Dalvi-Garcia, Luis L. Fonseca.

Project administration: Ana Tereza R. Vasconcelos, Eberhard O. Voit.

Resources: Ana Tereza R. Vasconcelos, Cecilia Hedin-Pereira, Eberhard O. Voit.

Software: Felipe Dalvi-Garcia.

Supervision: Luis L. Fonseca, Ana Tereza R. Vasconcelos, Cecilia Hedin-Pereira, Eberhard O. Voit.

Validation: Felipe Dalvi-Garcia.

Visualization: Felipe Dalvi-Garcia, Luis L. Fonseca.

Writing – original draft: Felipe Dalvi-Garcia, Luis L. Fonseca, Ana Tereza R. Vasconcelos, Cecilia Hedin-Pereira, Eberhard O. Voit.

Writing – review & editing: Felipe Dalvi-Garcia, Luis L. Fonseca, Ana Tereza R. Vasconcelos, Cecilia Hedin-Pereira, Eberhard O. Voit.

References

1. Association AP, others. Diagnostic and statistical manual of mental disorders (DSM-5®). American Psychiatric Pub; 2013.

2. World Health Organization. Depression and other common mental disorders: global health estimates. 2017;

3. Reddy M. Depression-the global crisis. Indian J Psychol Med. 2012; 34(3):201. https://doi.org/10.4103/0253-7176.106011 PMID: 23436954

4. Goldston K, Baillie AJ. Depression and coronary heart disease: a review of the epidemiological evidence, explanatory mechanisms and management approaches. Clin Psychol Rev. 2008; 28(2):288–306. https://doi.org/10.1016/j.cpr.2007.05.005 PMID: 17601644

5. Mezuk B, Eaton WW, Albrecht S, Golden SH. Depression and type 2 diabetes over the lifespan: a meta-analysis. Diabetes Care. 2008; 31(12):2383–90. https://doi.org/10.2337/dc08-0985 PMID: 19033418

6. Caraci F, Copani A, Nicoletti F, Drago F. Depression and Alzheimer's disease: neurobiological links and common pharmacological targets. Eur J Pharmacol. 2010; 626(1):64–71. https://doi.org/10.1016/j.ejphar.2009.10.022 PMID: 19837057

7. Monroe SM, Harkness KL. Recurrence in major depression: a conceptual analysis. Psychol Rev. 2011; 118(4):655. https://doi.org/10.1037/a0025190 PMID: 21895384

8. Slavich GM, Irwin MR. From stress to inflammation and major depressive disorder: a social signal transduction theory of depression. Psychol Bull. 2014; 140(3):774. https://doi.org/10.1037/a0035302 PMID: 24417575

9. Verduijn J, Milaneschi Y, Schoevers RA, van Hemert AM, Beekman ATF, Penninx BWJH. Pathophysiology of major depressive disorder: mechanisms involved in etiology are not associated with clinical progression. Transl Psychiatry. 2015; 5(9):e649–e649. https://doi.org/10.1038/tp.2015.137 PMID: 26418277

10. Herrmann N, Lanctôt KL, Khan LR. The role of norepinephrine in the behavioral and psychological symptoms of dementia. J Neuropsychiatry Clin Neurosci. 2004; 16(3):261–76. https://doi.org/10.1176/jnp.16.3.261 PMID: 15377733

11. Oades RD, Sadile AG, Sagvolden T, Viggiano D, Zuddas A, Devoto P, et al. The control of responsiveness in ADHD by catecholamines: evidence for dopaminergic, noradrenergic and interactive roles. Dev Sci. 2005; 8(2):122–31. https://doi.org/10.1111/j.1467-7687.2005.00399.x PMID: 15720370

12. Sánchez MG, Bourque M, Morissette M, Di Paolo T. Steroids-Dopamine Interactions in the Pathophysiology and Treatment of CNS Disorders. CNS Neurosci Ther. 2010; 16(3). https://doi.org/10.1111/j.1755-5949.2010.00163.x PMID: 20557567

13. Sghendo L, Mifsud J. Understanding the molecular pharmacology of the serotonergic system: using fluoxetine as a model. J Pharm Pharmacol. 2012; 64(3):317–25. https://doi.org/10.1111/j.2042-7158.2011.01384.x PMID: 22309263

14. Czéh B, Fuchs E, Wiborg O, Simon M. Animal models of major depression and their clinical implications. Prog Neuropsychopharmacol Biol Psychiatry. 2016; 64:293–310. https://doi.org/10.1016/j.pnpbp.2015.04.004 PMID: 25891248

15. Qi Z, Fieni D, Tretter F, Voit EO. The neurochemical mobile with non-linear interaction matrix: an exploratory computational model. Pharmacopsychiatry. 2013; 46(S 01):S53–S63. https://doi.org/10.1055/s-0033-1337920 PMID: 23599246

16. Qi Z, Gina PY, Tretter F, Pogarell O, Grace AA, Voit EO. A heuristic model for working memory deficit in schizophrenia. Biochim Biophys Acta Gen Subj. 2016; 1860(11):2696–705. https://doi.org/10.1016/j.bbagen.2016.04.031 PMID: 27177811

17. Anacker C, Zunszain PA, Carvalho LA, Pariante CM. The glucocorticoid receptor: pivot of depression and of antidepressant treatment? Psychoneuroendocrinology. 2011; 36(3):415–25. https://doi.org/10.1016/j.psyneuen.2010.03.007 PMID: 20399565

18. Albert PR, Vahid-Ansari F, Luckhart C. Serotonin-prefrontal cortical circuitry in anxiety and depression phenotypes: pivotal role of pre-and post-synaptic 5-HT1A receptor expression. Front Behav Neurosci. 2014; 8:199. https://doi.org/10.3389/fnbeh.2014.00199 PMID: 24936175

19. Siesser WB, Zhang X, Jacobsen JPR, Sotnikova TD, Gainetdinov RR, Caron MG. Tryptophan hydroxylase 2 genotype determines brain serotonin synthesis but not tissue content in C57Bl/6 and BALB/c congenic mice. Neurosci Lett. 2010; 481(1):6–11. https://doi.org/10.1016/j.neulet.2010.06.035 PMID: 20600620

20. Davey CG, Yücel M, Allen NB. The emergence of depression in adolescence: development of the prefrontal cortex and the representation of reward. Neurosci Biobehav Rev. 2008; 32(1):1–19. https://doi.org/10.1016/j.neubiorev.2007.04.016 PMID: 17570526

21. Ryding E, Lindström M, Träskman-Bendz L. The role of dopamine and serotonin in suicidal behaviour and aggression. Prog Brain Res. 2008; 172:307–15. https://doi.org/10.1016/S0079-6123(08)00915-1 PMID: 18772039

22. Oxenkrug G. Serotonin–kynurenine hypothesis of depression: historical overview and recent developments. Curr Drug Deliv. 2013; 14(5):514–21. https://doi.org/10.2174/1389450111314050002 PMID: 23514379

23. Lodish H, Berk A, Zipursky SL, Matsudaira P, Baltimore D, Darnell J, et al. Molecular cell biology. Vol. 3. WH Freeman New York; 1995.

24. Davis I, Liu A. What is the tryptophan kynurenine pathway and why is it important to neurotherapeutics? Vol. 15, Expert Rev Neurother. Taylor & Francis; 2015. p. 719–21. https://doi.org/10.1586/14737175.2015.1049999 PMID: 26004930

25. Stone TW. Neuropharmacology of quinolinic and kynurenic acids. Pharmacol Rev. 1993; 45(3):309–79. PMID: 8248282

26. Badawy AA-B, Morgan CJ. Tryptophan metabolites as potent inhibitors of aldehyde dehydrogenase activity and potential alcoholism-aversion therapeutic agents. In: International Congress Series. 2007. p. 344–51. https://doi.org/10.1016/j.ics.2007.07.020

27. Inoue T, Koyama T. Effects of acute and chronic administration of high-dose corticosterone and dexamethasone on regional brain dopamine and serotonin metabolism in rats. Prog Neuropsychopharmacol Biol Psychiatry. 1996; 20(1):147–56. https://doi.org/10.1016/0278-5846(95)00299-5 PMID: 8861184

28. Zhao Y, Ma R, Shen J, Su H, Xing D, Du L. A mouse model of depression induced by repeated corticosterone injections. Eur J Pharmacol. 2008; 581(1–2):113–20. https://doi.org/10.1016/j.ejphar.2007.12.005 PMID: 18184609

29. Festing S, Wilkinson R. The ethics of animal research: talking point on the use of animals in scientific research. EMBO Rep. 2007; 8(6):526–30. https://doi.org/10.1038/sj.embor.7400993 PMID: 17545991

30. Voit EO. Computational analysis of biochemical systems: a practical guide for biochemists and molecular biologists. Cambridge University Press; 2000.

31. Voit EO. Biochemical Systems Theory: A Review. ISRN Biomath. 2013; 2013:1–53. https://doi.org/10.1155/2013/897658

32. Lohr KM, Bernstein AI, Stout KA, Dunn AR, Lazo CR, Alter SP, et al. Increased vesicular monoamine transporter enhances dopamine release and opposes Parkinson disease-related neurodegeneration

in vivo. Proc Natl Acad Sci USA. 2014;201402134. https://doi.org/10.1073/pnas.1402134111 PMID: 24979780

33. Qi Z, Miller GW, Voit EO. A mathematical model of presynaptic dopamine homeostasis: implications for schizophrenia. Pharmacopsychiatry. 2008; 41(S 01):S89–S98.

34. Popova NK, Gilinsky MA, Amstislavskaya TG, Morosova EA, Seif I, De Maeyer E. Effect of MAO A knockout on catecholamines in mouse brain regions: Dopamine and norepinephrine in the cortex are unaffected by MAO A deficiency. Biog Amin. 2005;

35. Chen K, Holschneider DP, Wu W, Rebrin I, Shih JC. A spontaneous point mutation produces monoamine oxidase A/B knock-out mice with greatly elevated monoamines and anxiety-like behavior. J Biol Chem. 2004; 279(38):39645–52. https://doi.org/10.1074/jbc.M405550200 PMID: 15272015

36. Heikkila RE, Manzino L, Cabbat FS, Duvoisin RC. Protection against the dopaminergic neurotoxicity of 1-methyl-4-phenyl-1, 2, 5, 6-tetrahydropyridine by monoamine oxidase inhibitors. Nature. 1984; 311 (5985):467. https://doi.org/10.1038/311467a0 PMID: 6332989

37. Fox MA, Panessiti MG, Hall FS, Uhl GR, Murphy DL. An evaluation of the serotonin system and perseverative, compulsive, stereotypical, and hyperactive behaviors in dopamine transporter (DAT) knockout mice. Psychopharmacology (Berl). 2013; 227(4):685–95. https://doi.org/10.1007/s00213-013-2988-x PMID: 23417514

38. Fox MA, Panessiti MG, Moya PR, Tolliver TJ, Chen K, Shih JC, et al. Mutations in monoamine oxidase (MAO) genes in mice lead to hypersensitivity to serotonin-enhancing drugs: Implications for drug side effects in humans. Pharmacogenomics J. 2013; https://doi.org/10.1038/tpj.2012.35 PMID: 22964922

39. Huotari M, Gogos JA, Karayiorgou M, Koponen O, Forsberg M, Raasmaja A, et al. Brain catecholamine metabolism in catechol-O-methyltransferase (COMT)-deficient mice. Eur J Neurosci. 2002; 15 (2):246–56. https://doi.org/10.1046/j.0953-816x.2001.01856.x PMID: 11849292

40. Käenmäki M, Tammimäki A, Myöhänen T, Pakarinen K, Amberg C, Karayiorgou M, et al. Quantitative role of COMT in dopamine clearance in the prefrontal cortex of freely moving mice. J Neurochem. 2010; https://doi.org/10.1111/j.1471-4159.2010.06889.x PMID: 20626558

41. Gogos JA, Morgan M, Luine V, Santha M, Ogawa S, Pfaff D, et al. Catechol-O-methyltransferase-deficient mice exhibit sexually dimorphic changes in catecholamine levels and behavior. Proc Natl Acad Sci USA. 1998; 95(17):9991–6. https://doi.org/10.1073/pnas.95.17.9991 PMID: 9707588

42. Gainetdinov RR, Jones SR, Fumagalli F, Wightman RM, Caron MG. Re-evaluation of the role of the dopamine transporter in dopamine system homeostasis. Brain Res Rev. 1998; 26(2–3):148–53. https://doi.org/10.1016/s0165-0173(97)00063-5 PMID: 9651511

43. Mathews TA, Fedele DE, Coppelli FM, Avila AM, Murphy DL, Andrews AM. Gene dose-dependent alterations in extraneuronal serotonin but not dopamine in mice with reduced serotonin transporter expression. J Neurosci Methods. 2004; 140(1–2):169–81. https://doi.org/10.1016/j.jneumeth.2004.05.017 PMID: 15589347

44. Shen HW, Hagino Y, Kobayashi K, Shinohara-Tanaka K, Ikeda K, Yamamoto H, et al. Regional differences in extracellular dopamine and serotonin assessed by in vivo microdialysis in mice lacking dopamine and/or serotonin transporters. Neuropsychopharmacology. 2004; https://doi.org/10.1038/sj.npp.1300476 PMID: 15226739

45. Homberg JR, Olivier JDA, Smits BMG, Mul JD, Mudde J, Verheul M, et al. Characterization of the serotonin transporter knockout rat: A selective change in the functioning of the serotonergic system. Neuroscience. 2007; https://doi.org/10.1016/j.neuroscience.2007.03.030 PMID: 17467186

46. Jacobsen JPR, Siesser WB, Sachs BD, Peterson S, Cools MJ, Setola V, et al. Deficient serotonin neurotransmission and depression-like serotonin biomarker alterations in tryptophan hydroxylase 2 (Tph2) loss-of-function mice. Mol Psychiatry. 2012; https://doi.org/10.1038/mp.2011.50 PMID: 21537332

47. Reed MC, Frederik Nijhout H, Best JA. Mathematical insights into the effects of levodopa. Front Integr Neurosci. 2012; https://doi.org/10.3389/fnint.2012.00021 PMID: 22783173

48. Best JA, Nijhout HF, Reed MC. Homeostatic mechanisms in dopamine synthesis and release: a mathematical model. Theor Biol Med Model. 2009; 6(1):21. https://doi.org/10.1186/1742-4682-6-21 PMID: 19740446

49. Best JA, Nijhout HF, Reed M. Serotonin synthesis, release and reuptake in terminals: a mathematical model. Theor Biol Med Model. 2010; 7(1):34. https://doi.org/10.1186/1742-4682-7-34 PMID: 20723248

50. Best J, Duncan W, Sadre-Marandi F, Hashemi P, Nijhout HF, Reed M. Autoreceptor control of serotonin dynamics. BMC Neurosci. 2020; https://doi.org/10.1186/s12868-020-00587-z PMID: 32967609

51. Burke WJ, Kumar VB, Pandey N, Panneton WM, Gan Q, Franko MW, et al. Aggregation of α-synuclein by DOPAL, the monoamine oxidase metabolite of dopamine. Acta Neuropathol. 2008; 115(2):193–203. https://doi.org/10.1007/s00401-007-0303-9 PMID: 17965867

52. Jinsmaa Y, Cooney A, Sullivan P, Sharabi Y, Goldstein DS. The serotonin aldehyde, 5-HIAL, oligomerizes alpha-synuclein. Neurosci Lett. 2015; 590:134–7. https://doi.org/10.1016/j.neulet.2015.01.064 PMID: 25637699

53. Ishiguro M, Baba H, Maeshima H, Shimano T, Inoue M, Ichikawa T, et al. Increased serum levels of α-synuclein in patients with major depressive disorder. Am J Geriatr Psychiatry. 2018; https://doi.org/10.1016/j.jagp.2018.10.015 PMID: 30503177

54. Plotegher N, Berti G, Ferrari E, Tessari I, Zanetti M, Lunelli L, et al. DOPAL derived alpha-synuclein oligomers impair synaptic vesicles physiological function. Sci Rep. 2017; 7:40699. https://doi.org/10.1038/srep40699 PMID: 28084443

55. Culmsee C, Michels S, Scheu S, Arolt V, Dannlowski U, Alferink J. Mitochondria, Microglia, and the Immune System—How Are They Linked in Affective Disorders? Front Psychiatry. 2019; 9:739. https://doi.org/10.3389/fpsyt.2018.00739 PMID: 30687139

56. Rocha EM, De Miranda B, Sanders LH. Alpha-synuclein: pathology, mitochondrial dysfunction and neuroinflammation in Parkinson's disease. Neurobiol Dis. 2018; 109:249–57. https://doi.org/10.1016/j.nbd.2017.04.004 PMID: 28400134

57. Zhang W-Y, Wang K-Y, Li Y-J, Li Y-R, Lu R-Z. Chronic stress causes protein kinase C epsilon-aldehyde dehydrogenase 2 signaling pathway perturbation in the rat hippocampus and prefrontal cortex, but not in the myocardium. Neural Regen Res. 2018; 13(7):1225. https://doi.org/10.4103/1673-5374.235060 PMID: 30028331

58. Rees JN, Florang VR, Anderson DG, Doorn JA. Lipid peroxidation products inhibit dopamine catabolism yielding aberrant levels of a reactive intermediate. Chem Res Toxicol. 2007; 20(10):1536–42. https://doi.org/10.1021/tx700248y PMID: 17887726

59. Jinsmaa Y, Florang VR, Rees JN, Anderson DG, Strack S, Doorn JA. Products of oxidative stress inhibit aldehyde oxidation and reduction pathways in dopamine catabolism yielding elevated levels of a reactive intermediate. Chem Res Toxicol. 2009; 22(5):835–41. https://doi.org/10.1021/tx800405v PMID: 19388687

60. Salim S. Oxidative stress: a potential link between emotional wellbeing and immune response. Curr Opin Pharmacol. 2016; 29:70–6. https://doi.org/10.1016/j.coph.2016.06.006 PMID: 27400336

61. Stone TW, Burton NR. NMDA receptors and ligands in the vertebrate CNS. Prog Neurobiol. 1988; 30 (4):333–68. https://doi.org/10.1016/0301-0082(88)90027-5 PMID: 2830636

62. Tavares RG, Tasca CI, Santos CES, Wajner M, Souza DO, Dutra-Filho CS. Quinolinic acid inhibits glutamate uptake into synaptic vesicles from rat brain. Neuroreport. 2000; 11(2):249–54. https://doi.org/10.1097/00001756-200002070-00005 PMID: 10674464

63. Magariños AM, Verdugo JMG, McEwen BS. Chronic stress alters synaptic terminal structure in hippocampus. Proc Natl Acad Sci USA. 1997; 94(25):14002–8. https://doi.org/10.1073/pnas.94.25.14002 PMID: 9391142

64. Lupien SJ, de Leon M, De Santi S, Convit A, Tarshish C, Nair NP V, et al. Cortisol levels during human aging predict hippocampal atrophy and memory deficits. Nat Neurosci. 1998; 1(1):69. https://doi.org/10.1038/271 PMID: 10195112

65. Savitz J, Dantzer R, Wurfel BE, Victor TA, Ford BN, Bodurka J, et al. Neuroprotective kynurenine metabolite indices are abnormally reduced and positively associated with hippocampal and amygdalar volume in bipolar disorder. Psychoneuroendocrinology. 2015; 52:200–11. https://doi.org/10.1016/j.psyneuen.2014.11.015 PMID: 25486577

66. Savitz J, Drevets WC, Smith CM, Victor TA, Wurfel BE, Bellgowan PSF, et al. Putative neuroprotective and neurotoxic kynurenine pathway metabolites are associated with hippocampal and amygdalar volumes in subjects with major depressive disorder. Neuropsychopharmacology. 2015; 40(2):463. https://doi.org/10.1038/npp.2014.194 PMID: 25074636

67. Bellac CL, Coimbra RS, Christen S, Leib SL. Pneumococcal meningitis causes accumulation of neurotoxic kynurenine metabolites in brain regions prone to injury. Neurobiol Dis. 2006; 24(2):395–402. https://doi.org/10.1016/j.nbd.2006.07.014 PMID: 16956766

68. Monnerie H, Shashidhara S, Le Roux PD. Effect of excess extracellular glutamate on dendrite growth from cerebral cortical neurons at 3 days in vitro: Involvement of NMDA receptors. J Neurosci Res. 2003; 74(5):688–700. https://doi.org/10.1002/jnr.10797 PMID: 14635220

69. Herman JP, Cullinan WE. Neurocircuitry of stress: central control of the hypothalamo–pituitary–adrenocortical axis. Trends Neurosci. 1997; 20(2):78–84. https://doi.org/10.1016/s0166-2236(96)10069-2 PMID: 9023876

70. Frodl T, O'Keane V. How does the brain deal with cumulative stress? A review with focus on developmental stress, HPA axis function and hippocampal structure in humans. Neurobiol Dis. 2013; 52:24–37. https://doi.org/10.1016/j.nbd.2012.03.012 PMID: 22426398

71. MacQueen GM, Campbell S, McEwen BS, Macdonald K, Amano S, Joffe RT, et al. Course of illness, hippocampal function, and hippocampal volume in major depression. Proc Natl Acad Sci USA. 2003; 100(3):1387–92. https://doi.org/10.1073/pnas.0337481100 PMID: 12552118

72. Sheline YI, Gado MH, Kraemer HC. Untreated depression and hippocampal volume loss. Am J Psychiatry. 2003; 160(8):1516–8. https://doi.org/10.1176/appi.ajp.160.8.1516 PMID: 12900317

73. MacQueen G, Frodl T. The hippocampus in major depression: evidence for the convergence of the bench and bedside in psychiatric research? Mol Psychiatry. 2011; 16(3):252. https://doi.org/10.1038/mp.2010.80 PMID: 20661246

74. Martín-Hernández D, Tendilla-Beltrán H, Madrigal JLM, García-Bueno B, Leza JC, Caso JR. Chronic mild stress alters kynurenine pathways changing the glutamate neurotransmission in frontal cortex of Rats. Mol Neurobiol. 2019; 56(1):490–501. https://doi.org/10.1007/s12035-018-1096-7 PMID: 29725904

75. Schwarcz R, Bruno JP, Muchowski PJ, Wu H-Q. Kynurenines in the mammalian brain: when physiology meets pathology. Nat Rev Neurosci. 2012; 13(7):465. https://doi.org/10.1038/nrn3257 PMID: 22678511

76. Pearson SJ, Reynolds GP. Increased brain concentrations of a neurotoxin, 3-hydroxykynurenine, in Huntington's disease. Neurosci Lett. 1992; 144(1–2):199–201. https://doi.org/10.1016/0304-3940(92)90749-w PMID: 1436703

77. Moret C, Briley M. The importance of norepinephrine in depression. Neuropsychiatr Dis Treat [Internet]. 2011 May 31 [cited 2020 Aug 27]; 7(SUPPL.):9–13. Available from: /pmc/articles/PMC3131098/?report = abstract https://doi.org/10.2147/NDT.S19619 PMID: 21750623

78. Günther J, Däbritz J, Wirthgen E. Limitations and off-target effects of tryptophan-related IDO inhibitors in cancer treatment. Front Immunol. 2019; 10:1801. https://doi.org/10.3389/fimmu.2019.01801 PMID: 31417567

79. Stavrum A-K, Heiland I, Schuster S, Puntervoll P, Ziegler M. Model of tryptophan metabolism, readily scalable using tissue-specific gene expression data. J Biol Chem. 2013;jbc–M113. https://doi.org/10.1074/jbc.M113.474908 PMID: 24129579

80. Owe-Young R, Webster NL, Mukhtar M, Pomerantz RJ, Smythe G, Walker D, et al. Kynurenine pathway metabolism in human blood–brain–barrier cells: implications for immune tolerance & neurotoxicity. J Neurochem. 2008; 105(4):1346–57. https://doi.org/10.1111/j.1471-4159.2008.05241.x PMID: 18221377

81. Schomburg I, Chang A, Schomburg D. BRENDA, enzyme data and metabolic information. Nucleic Acids Res. 2002; 30(1):47–9. https://doi.org/10.1093/nar/30.1.47 PMID: 11752250

82. Kanehisa M, Goto S. KEGG: kyoto encyclopedia of genes and genomes. Nucleic Acids Res. 2000; 28 (1):27–30. https://doi.org/10.1093/nar/28.1.27 PMID: 10592173

83. Karp PD, Riley M, Paley SM, Pellegrini-Toole A. The metacyc database. Nucleic Acids Res. 2002; 30 (1):59–61. https://doi.org/10.1093/nar/30.1.59 PMID: 11752254

84. Guillemin GJ, Kerr SJ, Smythe GA, Smith DG, Kapoor V, Armati PJ, et al. Kynurenine pathway metabolism in human astrocytes: a paradox for neuronal protection. J Neurochem. 2001; 78(4):842–53. https://doi.org/10.1046/j.1471-4159.2001.00498.x PMID: 11520905

85. Guillemin GJ, Smith DG, Smythe GA, Armati PJ, Brew GJ. Expression of the kynurenine pathway enzymes in human microglia and macrophages. In: Developments in Tryptophan and Serotonin Metabolism. Springer; 2003. p. 105–12. https://doi.org/10.1007/978-1-4615-0135-0_12 PMID: 15206722

86. Abbott NJ, Patabendige AAK, Dolman DEM, Yusof SR, Begley DJ. Structure and function of the blood–brain barrier. Neurobiol Dis. 2010; 37(1):13–25. https://doi.org/10.1016/j.nbd.2009.07.030 PMID: 19664713

87. Hawkins RA, O'kane RL, Simpson IA, Vina JR. Structure of the blood–brain barrier and its role in the transport of amino acids. J Nutr. 2006; 136(1):218S–226S. https://doi.org/10.1093/jn/136.1.218S PMID: 16365086

88. Pardridge WM. Blood-brain barrier drug targeting: the future of brain drug development. Mol Interv. 2003; 3(2):90. https://doi.org/10.1124/mi.3.2.90 PMID: 14993430

89. O'Kane RL, Hawkins RA. Na+-dependent transport of large neutral amino acids occurs at the abluminal membrane of the blood-brain barrier. Am J Physiol Endocrinol Metab. 2003; 285(6):E1167–E1173. https://doi.org/10.1152/ajpendo.00193.2003 PMID: 12933350

90. Fotiadis D, Kanai Y, Palac\'\in M. The SLC3 and SLC7 families of amino acid transporters. Mol Asp Med. 2013; 34(2–3):139–58. https://doi.org/10.1016/j.mam.2012.10.007 PMID: 23506863

91. Fernstrom JD. Large neutral amino acids: dietary effects on brain neurochemistry and function. Amin acids. 2013; 45(3):419–30. https://doi.org/10.1007/s00726-012-1330-y PMID: 22677921

92. Koyanagi T, Nakagawa A, Sakurama H, Yamamoto K, Sakurai N, Takagi Y, et al. Eukaryotic-type aromatic amino acid decarboxylase from the root colonizer Pseudomonas putida is highly specific for 3, 4-dihydroxyphenyl-L-alanine, an allelochemical in the rhizosphere. Microbiology. 2012; 158(12):2965–74. https://doi.org/10.1099/mic.0.062463-0 PMID: 23059975

93. Roberts KM, Fitzpatrick PF. Mechanisms of tryptophan and tyrosine hydroxylase. IUBMB Life. 2013; 65(4):350–7. https://doi.org/10.1002/iub.1144 PMID: 23441081

94. Zhu H, Xu G, Zhang K, Kong X, Han R, Zhou J, et al. Crystal structure of tyrosine decarboxylase and identification of key residues involved in conformational swing and substrate binding. Sci Rep. 2016; 6:27779. https://doi.org/10.1038/srep27779 PMID: 27292129

95. Doyle D. The fine structure of the nervous system: the neurons and supporting cells. J Neurol Neurosurg Psychiatry. 1978; 41(2):191.

96. Floor E, Schaeffer SF, Feist BE, Leeman SE. Synaptic vesicles from mammalian brain: Large-scale purification and physical and immunochemical characterization. J Neurochem. 1988; 50(5):1588–96. https://doi.org/10.1111/j.1471-4159.1988.tb03048.x PMID: 3361314

97. Kim S, Atwood HL, Cooper RL. Assessing accurate sizes of synaptic vesicles in nerve terminals. Brain Res. 2000; 877(2):209–17. https://doi.org/10.1016/s0006-8993(00)02641-x PMID: 10986334

98. Südhof TC. The synaptic vesicle cycle: a cascade of protein–protein interactions. Nature. 1995; 375 (6533):645. https://doi.org/10.1038/375645a0 PMID: 7791897

99. Lei Y, Han H, Yuan F, Javeed A, Zhao Y. The brain interstitial system: Anatomy, modeling, in vivo measurement, and applications. Prog Neurobiol. 2017; 157:230–46. https://doi.org/10.1016/j.pneurobio.2015.12.007 PMID: 26837044

100. Reinoso RF, Telfer BA, Rowland M. Tissue water content in rats measured by desiccation. J Pharmacol Toxicol Methods. 1997; 38(2):87–92. https://doi.org/10.1016/s1056-8719(97)00053-1 PMID: 9403779

101. Banks WA. Characteristics of compounds that cross the blood-brain barrier. In: BMC neurology. 2009. p. S3. https://doi.org/10.1186/1471-2377-9-S1-S3 PMID: 19534732

102. El-Farhan N, Rees DA, Evans C. Measuring cortisol in serum, urine and saliva–are our assays good enough? Ann Clin Biochem. 2017; 54(3):308–22. https://doi.org/10.1177/0004563216687335 PMID: 28068807

103. Murphy BEP. Steroids and depression. J Steroid Biochem Mol Biol. 1991; 38(5):537–59. https://doi.org/10.1016/0960-0760(91)90312-s PMID: 1645586

104. Alexandraki KI, Grossman AB. Is urinary free cortisol of value in the diagnosis of Cushing's syndrome? Curr Opin Endocrinol Diabetes Obes. 2011; 18(4):259–63. https://doi.org/10.1097/MED.0b013e3283487193 PMID: 21681089

105. Edfors F, Danielsson F, Hallström BM, Käll L, Lundberg E, Pontén F, et al. Gene-specific correlation of RNA and protein levels in human cells and tissues. Mol Syst Biol. 2016; 12(10):883. https://doi.org/10.15252/msb.20167144 PMID: 27951527

106. Schwanhäusser B, Busse D, Li N, Dittmar G, Schuchhardt J, Wolf J, et al. Global quantification of mammalian gene expression control. Nature. 2011; 473(7347):337–42. https://doi.org/10.1038/nature10098 PMID: 21593866

107. Reiche EMV, Nunes SOV, Morimoto HK. Stress, depression, the immune system, and cancer. Lancet Oncol. 2004; 5(10):617–25. https://doi.org/10.1016/S1470-2045(04)01597-9 PMID: 15465465

108. Schleimer RP. An overview of glucocorticoid anti-inflammatory actions. Eur J Clin Pharmacol. 1993; 45(1):S3–S7. https://doi.org/10.1007/BF01844196 PMID: 8313932

109. Himmerich H, Fulda S, Linseisen J, Seiler H, Wolfram G, Himmerich S, et al. Depression, comorbidities and the TNF-α system. Eur Psychiatry. 2008 Sep 1; 23(6):421–9. https://doi.org/10.1016/j.eurpsy.2008.03.013 PMID: 18504118

110. Cumming P, Ase A, Kuwabara H, Gjedde A. [3H] DOPA formed from [3H] tyrosine in living rat brain is not committed to dopamine synthesis. J Cereb Blood Flow Metab. 1998; 18(5):491–9. https://doi.org/10.1097/00004647-199805000-00004 PMID: 9591841

111. Nakamura K, Hasegawa H. Production and peripheral roles of 5-HTP, a precursor of serotonin. Int J Tryptophan Res. 2009; 2:IJTR–S1022. https://doi.org/10.4137/ijtr.s1022 PMID: 22084581

112. Mokler DJ, Torres OI, Galler JR, Morgane PJ. Stress-induced changes in extracellular dopamine and serotonin in the medial prefrontal cortex and dorsal hippocampus of prenatally malnourished rats. Brain Res. 2007; 1148:226–33. https://doi.org/10.1016/j.brainres.2007.02.031 PMID: 17368432

113. Pozzi L, Invernizzi R, Garavaglia C, Samanin R. Fluoxetine increases extracellular dopamine in the prefrontal cortex by a mechanism not dependent on serotonin. J Neurochem. 1999; 73(3):1051–7. https://doi.org/10.1046/j.1471-4159.1999.0731051.x PMID: 10461894

114. Tanda G, Carboni E, Frau R, Di Chiara G. Increase of extracellular dopamine in the prefrontal cortex: a trait of drugs with antidepressant potential? Psychopharmacology (Berl). 1994; 115(1–2):285–8. https://doi.org/10.1007/BF02244785 PMID: 7862908

115. Tanda G, Frau R, Di Chiara G. Chronic desipramine and fluoxetine differentially affect extracellular dopamine in the rat prefrontal cortex. Psychopharmacology (Berl). 1996; 127(1–2):83–7. https://doi.org/10.1007/BF02805978 PMID: 8888371

116. Carvalho MC, Albrechet-Souza L, Masson S, Brandão ML. Changes in the biogenic amine content of the prefrontal cortex, amygdala, dorsal hippocampus, and nucleus accumbens of rats submitted to single and repeated sessions of the elevated plus-maze test. Braz J Med Biol Res. 2005; 38(12):1857–66. https://doi.org/10.1590/s0100-879x2005001200014 PMID: 16302100

117. Mooslehner KA, Chan PM, Xu W, Liu L, Smadja C, Humby T, et al. Mice with very low expression of the vesicular monoamine transporter 2 gene survive into adulthood: potential mouse model for parkinsonism. Mol Cell Biol. 2001; 21(16):5321–31. https://doi.org/10.1128/MCB.21.16.5321-5331.2001 PMID: 11463816

118. Wolkowitz O, Sutton M, Koulo M, Labarca R, Wilkinson L, Doran A, et al. Chronic corticosterone administration in rats: behavioral and biochemical evidence of increased central dopaminergic activity. Eur J Pharmacol. 1986; 122(3):329–38. https://doi.org/10.1016/0014-2999(86)90413-9 PMID: 3709658

119. Adell A, Carceller A, Artigas F. Regional distribution of extracellular 5-hydroxytryptamine and 5-hydroxyindoleacetic acid in the brain of freely moving rats. J Neurochem. 1991; 56(2):709–12. https://doi.org/10.1111/j.1471-4159.1991.tb08208.x PMID: 1703223

120. Miyamoto JK, Uezu E, Yusa T, Terashima S-I. Efflux of 5-HIAA form 5-HT neurons: A membrane potential-dependent process. Physiol Behav. 1990; 47(4):767–72. https://doi.org/10.1016/0031-9384(90)90092-i PMID: 1696745

121. Burke WJ, Chung HD, Li SW. Quantitation of 3, 4-dihydroxyphenylacetaldehyde and 3, 4-dihydroxyphenylglycolaldehyde, the monoamine oxidase metabolites of dopamine and noradrenaline, in human tissues by microcolumn high-performance liquid chromatography. Anal Biochem. 1999; 273(1):111–6. https://doi.org/10.1006/abio.1999.4196 PMID: 10452806

122. Ribeiro P, Pigeon D, Kaufman S. The hydroxylation of phenylalanine and tyrosine by tyrosine hydroxylase from cultured pheochromocytoma cells. J Biol Chem. 1991; 266(24):16207–11. PMID: 1678741

123. Ribeiro P, Wang Y, Citron BA, Kaufman S. Regulation of recombinant rat tyrosine hydroxylase by dopamine. Proc Natl Acad Sci USA. 1992; 89(20):9593–7. https://doi.org/10.1073/pnas.89.20.9593 PMID: 1357665

124. Norrholm SD, Horton DB, Dwoskin LP. The promiscuity of the dopamine transporter: Implications for the kinetic analysis of [3H]serotonin uptake in rat hippocampal and striatal synaptosomes. Neuropharmacology. 2007; https://doi.org/10.1016/j.neuropharm.2007.10.001 PMID: 18022203

125. Daws LC. Unfaithful neurotransmitter transporters: Focus on serotonin uptake and implications for antidepressant efficacy. Pharmacology and Therapeutics. 2009. https://doi.org/10.1016/j.pharmthera.2008.10.004 PMID: 19022290

126. Larsen MB, Sonders MS, Mortensen OV, Larson GA, Zahniser NR, Amara SG. Dopamine transport by the serotonin transporter: A Mechanistically distinct mode of substrate translocation. J Neurosci. 2011; https://doi.org/10.1523/JNEUROSCI.0576-11.2011 PMID: 21525301

127. Bowling KM, Huang Z, Xu D, Ferdousy F, Funderburk CD, Karnik N, et al. Direct binding of GTP cyclohydrolase and tyrosine hydroxylase: Regulatory interactions between key enzymes in dopamine biosynthesis. J Biol Chem. 2008; https://doi.org/10.1074/jbc.M802552200 PMID: 18801743

128. Cartier EA, Parra LA, Baust TB, Quiroz M, Salazar G, Faundez V, et al. A biochemical and functional protein complex involving dopamine synthesis and transport into synaptic vesicles. J Biol Chem. 2010; https://doi.org/10.1074/jbc.M109.054510 PMID: 19903816

129. Doorn JA, Florang VR, Schamp JH, Vanle BC. Aldehyde dehydrogenase inhibition generates a reactive dopamine metabolite autotoxic to dopamine neurons. Park Relat Disord. 2014; 20:S73–S75. https://doi.org/10.1016/S1353-8020(13)70019-1 PMID: 24262193

130. Filipenko ML, Beilina AG, Alekseyenko O V, Dolgov V V, Kudryavtseva NN. Repeated experience of social defeats increases serotonin transporter and monoamine oxidase A mRNA levels in raphe nuclei

of male mice. Neurosci Lett. 2002; 321(1–2):25–8. https://doi.org/10.1016/s0304-3940(01)02495-8 PMID: 11872248

131. Grunewald M, Johnson S, Lu D, Wang Z, Lomberk G, Albert PR, et al. Mechanistic role for a novel glucocorticoid-KLF11 (TIEG2) protein pathway in stress-induced monoamine oxidase A expression. J Biol Chem. 2012; 287(29):24195–206. https://doi.org/10.1074/jbc.M112.373936 PMID: 22628545

132. Slotkin TA, Seidler FJ, Ritchie JC. Effects of aging and glucocorticoid treatment on monoamine oxidase subtypes in rat cerebral cortex: therapeutic implications. Brain Res Bull. 1998; 47(4):345–8. https://doi.org/10.1016/s0361-9230(98)00111-7 PMID: 9886786

133. Liao M, Pabarcus MK, Wang Y, Hefner C, Maltby DA, Medzihradszky KF, et al. Impaired dexamethasone-mediated induction of tryptophan 2, 3-dioxygenase in heme-deficient rat hepatocytes: translational control by a hepatic eIF2α kinase, the heme-regulated inhibitor. J Pharmacol Exp Ther. 2007; 323(3):979–89. https://doi.org/10.1124/jpet.107.124602 PMID: 17761498

134. Stone TW, Darlington LG. The kynurenine pathway as a therapeutic target in cognitive and neurodegenerative disorders. Br J Pharmacol. 2013; 169(6):1211–27. https://doi.org/10.1111/bph.12230 PMID: 23647169

135. Wichers MC, Maes M. The role of indoleamine 2, 3-dioxygenase (IDO) in the pathophysiology of interferon-α-induced depression. J Psychiatry Neurosci. 2004; 29(1):11. PMID: 14719046

136. Chen Y, Xu H, Zhu M, Liu K, Lin B, Luo R, et al. Stress inhibits tryptophan hydroxylase expression in a rat model of depression. Oncotarget. 2017; 8(38):63247. https://doi.org/10.18632/oncotarget.18780 PMID: 28968985

137. Chrousos GP. The hypothalamic–pituitary–adrenal axis and immune-mediated inflammation. N Engl J Med. 1995; 332(20):1351–63. https://doi.org/10.1056/NEJM199505183322008 PMID: 7715646

138. Voit EO. Models-of-data and models-of-processes in the post-genomic era. Math Biosci. 2002; https://doi.org/10.1016/s0025-5564(02)00115-3 PMID: 12387927

139. Savageau MA. Biochemical systems analysis: I. Some mathematical properties of the rate law for the component enzymatic reactions. J Theor Biol. 1969; 25(3):365–9. https://doi.org/10.1016/s0022-5193(69)80026-3 PMID: 5387046

140. Savageau MA. Biochemical systems analysis: II. The steady-state solutions for an n-pool system using a power-law approximation. J Theor Biol. 1969; 25(3):370–9. https://doi.org/10.1016/s0022-5193(69)80027-5 PMID: 5387047

141. Savageau MA. Biochemical systems analysis. A study of function and design in molecular biology. In: Addison Wesley Publ. 1976.

142. Torres N V, Voit EO. Pathway analysis and optimization in metabolic engineering. Cambridge University Press; 2002.

143. Voit EO, Martens HA, Omholt SW. 150 Years of the Mass Action Law. PLoS Comput Biol. 2015; https://doi.org/10.1371/journal.pcbi.1004012 PMID: 25569257

144. Savageau MA. Development of fractal kinetic theory for enzyme-catalysed reactions and implications for the design of biochemical pathways. Biosystems. 1998; 47(1–2):9–36. https://doi.org/10.1016/s0303-2647(98)00020-3 PMID: 9715749

145. Bajzer Ž, Huzak M, Neff KL, Prendergast FG. Mathematical analysis of models for reaction kinetics in intracellular environments. Math Biosci. 2008; 215(1):35–47. https://doi.org/10.1016/j.mbs.2008.05.003 PMID: 18597792

146. Neff KL, Offord CP, Caride AJ, Strehler EE, Prendergast FG, Bajzer Ž. Validation of fractal-like kinetic models by time-resolved binding kinetics of dansylamide and carbonic anhydrase in crowded media. Biophys J. 2011; 100(10):2495–503. https://doi.org/10.1016/j.bpj.2011.04.016 PMID: 21575584

147. Voit EO. The best models of metabolism. Wiley Interdiscip Rev Syst Biol Med [Internet]. 2017 Nov 1 [cited 2020 Sep 1]; 9(6):e1391. Available from: http://doi.wiley.com/10.1002/wsbm.1391

148. Curto R, Sorribas A, Cascante M. Comparative characterization of the fermentation pathway of Saccharomyces cerevisiae using biochemical systems theory and metabolic control analysis: model definition and nomenclature. Math Biosci. 1995; 130(1):25–50. https://doi.org/10.1016/0025-5564(94)00092-e PMID: 7579901

149. Curto R, Voit EO, Sorribas A, Cascante M. Mathematical models of purine metabolism in man. Math Biosci. 1998; 151(1):1–49. https://doi.org/10.1016/s0025-5564(98)10001-9 PMID: 9664759

150. Alvarez-Vasquez F, Sims KJ, Hannun YA, Voit EO. Integration of kinetic information on yeast sphingolipid metabolism in dynamical pathway models. J Theor Biol. 2004; 226(3):265–91. https://doi.org/10.1016/j.jtbi.2003.08.010 PMID: 14643642

151. Savageau MA, Voit EO. Recasting nonlinear differential equations as S-systems: a canonical nonlinear form. Math Biosci. 1987; 87(1):83–115. https://doi.org/10.1016/0025-5564(87)90035-6

152.   Sims KJ, Alvarez-Vasquez F, Voit EO, Hannun YA. A guide to biochemical systems modeling of sphingolipids for the biochemist. Meth Enzym. 2007; 432:319–50. https://doi.org/10.1016/S0076-6879(07)32013-2 PMID: 17954223

153.   Marin-Sanguino A, Gupta SK, Voit EO, Vera J. Biochemical pathway modeling tools for drug target detection in cancer and other complex diseases. In: Meth Enzymol. Elsevier; 2011. p. 319–69. https://doi.org/10.1016/B978-0-12-381270-4.00011-1 PMID: 21187230

154.   Chou IC, Voit EO. Recent developments in parameter estimation and structure identification of biochemical and genomic systems. Mathematical Biosciences. 2009. https://doi.org/10.1016/j.mbs.2009.03.002 PMID: 19327372

155.   Rios-Avila L, Nijhout HF, Reed MC, Sitren HS, Gregory JF III. A mathematical model of tryptophan metabolism via the kynurenine pathway provides insights into the effects of vitamin B-6 deficiency, tryptophan loading, and induction of tryptophan 2, 3-dioxygenase on tryptophan metabolites. J Nutr. 2013; 143(9):1509–19. https://doi.org/10.3945/jn.113.174599 PMID: 23902960

156.   McKay MD, Beckman RJ, Conover WJ. Comparison of three methods for selecting values of input variables in the analysis of output from a computer code. Technometrics. 1979; 21(2):239–45. https://doi.org/10.2307/1268522

157.   Lagarias JC, Reeds JA, Wright MH, Wright PE. Convergence properties of the Nelder–Mead simplex method in low dimensions. SIAM J Optim. 1998; 9(1):112–47. https://doi.org/10.1137/S1052623496303470

158.   Deutch AY, Roth RH. The determinants of stress-induced activation of the prefrontal cortical dopamine system. In: Prog Brain Res. Elsevier; 1991. p. 367–403. https://doi.org/10.1016/S0079-6123(08)62691-6 PMID: 2094906